NATIONAL TECHNICAL UNIVERSITY OF ATHENS
INTERDISCIPLINARY POSTGRADUATE SPECIALIZATION PROGRAMME
"AUTOMATION SYSTEMS"
SCHOOL OF MECHANICAL ENGINEERING

Distributed Control Protocols for Vehicular Platoons

Master Thesis

of

CHRISTOS K. VERGINIS

Supervisor: Kostas J. Kyriakopoulos
Professor

Athens, September 2015

NATIONAL TECHNICAL UNIVERSITY OF ATHENS
INTERDISCIPLINARY POSTGRADUATE SPECIALIZATION PROGRAMME
”AUTOMATION SYSTEMS”
SCHOOL OF MECHANICAL ENGINEERING

Distributed Control Protocols for Vehicular Platoons

Master Thesis

of

CHRISTOS K. VERGINIS

Supervisor: Kostas J. Kyriakopoulos
Professor

Approved by the three-member committee in .... 2015.

(Signature)	*(Signature)*	*(Signature)*
....	....	....
Kostas J. Kyriakopoulos Professor	Costas S. Tzafestas Associate Professor	Evangelos Papadopoulos Professor

Athens, September 2015

NATIONAL TECHNICAL UNIVERSITY OF ATHENS
INTERDISCIPLINARY POSTGRADUATE SPECIALIZATION PROGRAMME
”AUTOMATION SYSTEMS”
SCHOOL OF MECHANICAL ENGINEERING

Copyright © – All rights reserved.
CHRISTOS VERGINIS, 2015.

(Signature)

. . . .
C. VERGINIS

Περίληψη

Στην παρούσα εργασία μελετούμε το πρόβλημα ελέγχου της διάταξης για φάλαγγες οχημάτων με άγνωστο δυναμικό μοντέλο, που κινούνται σε μονοδιάστατους και δι-διάστατους χώρους. Πιο συγκεκριμένα, σχεδιάζουμε ένα αποκεντρωμένο πρωτόκολλο ελέγχου υπό την έννοια ότι κάθε όχημα χρησιμοποιεί μόνο τοπικές σχετικές πληροφορίες αναφορικά με τα γειτονικά του οχήματα, τις οποίες λαμβάνει με κατάλληλους αισθητήρες, για να υπολογίσει το σήμα ελέγχου του, χωρίς να ενσωματώνει εκ των προτέρων γνώση μη γραμμικοτήτων του δυναμικού μοντέλου των οχημάτων ή εξωγενών διαταραχών. Επιπροσθέτως, η απόκριση μεταβατικής και μόνιμης κατάστασης προκαθορίζεται δια μέσου συγκεκριμένων κατάλληλα σχεδιασμένων συναρτήσεων επίδοσης και είναι πλήρως αποσυζευγμένη από το δυναμικό μοντέλο των πρακτόρων, τον αριθμό των οχημάτων που αποτελούν τη φάλαγγα και την επιλογή των κερδών ελέγχου, γεγονός το οποίο χαλαρώνει σημαντικά τη διαδικασία σχεδιασμού του ελεκτή. Επιπλέον, αποδεικνύεται ότι συγκρούσεις μεταξύ διαδοχικών οχημάτων καθώς και διακοπές συνδεσιμότητας λόγω περιορισμένων δυνατοτήτων των αισθητήρων αποφεύγονται. Τέλος, η αποδοτικότητα και επίδοση των προτεινόμενων σχημάτων ελέγχου επαληθεύονται μέσω υπολογιστικών προσομοιώσεων και πειραμάτων σε πραγματικό χρόνο.

Λέξεις Κλειδιά

Ρομποτική, Μη Γραμμικός Έλεγχος, Φάλαγγες Οχημάτων, Οχήματα, Συναρτήσεις επίδοσης, Αποκεντρωμένος Έλεγχος, Διανεμημένα Πρωτόκολλα Ελέγχου

Abstract

In this work, we consider the formation control problem for vehicular platoons with unknown nonlinear dynamics operating in 1-dimensional and 2-dimensional Euclidean space. More specifically, we design a decentralized model-free control protocol in the sense that each vehicle utilizes only local relative information regarding its neighboring vehicles, obtained by its on-board sensors, to calculate its own control signal, without incorporating any prior knowledge of the model nonlinearities/disturbances or any approximation structures to acquire such knowledge. Additionally, the transient and steady state response is a priori determined by certain designer-specified performance functions and is fully decoupled by the agents' dynamic model, the number of vehicles composing the platoon and the control gains selection, which relaxes significantly the control design procedure. Moreover, collisions between successive vehicles as well as connectivity breaks owing to limited sensor capabilities are provably avoided. Finally, real-time experiments concering the 1-D case as well as extensive simulation studies for both cases clarify the proposed control schemes and verify their effectiveness.

Keywords

Robotics, Nonlinear Control, Platoon, Vehicular Platoon, Prescribed Performance, Decentralized Control, Distributed Control Protocol, Model-free Control

Contents

Περίληψη 1

Abstract 3

1 Introduction 9
  1.1 Purpose 9
  1.2 Bibliography Review 10
  1.3 Structure 12

2 Problem Statement 13
  2.1 1-Dimensional Case 13
  2.2 2-Dimensional Case 15

3 Main Results 19
  3.1 1-Dimensional Case 19
    3.1.1 Stability Analysis 22
    3.1.2 Simulations 27
  3.2 2-Dimensional Case 34
    3.2.1 Control Design 34
    3.2.2 Stability Analysis 37
    3.2.3 Simulations 43

4 Experimental Evaluation 49
  4.1 System Components 49
  4.2 Experimental Results 51

5 Conclusions and Future Work 55
  5.1 Conclusion 55
  5.2 Future Work 55

Appendices 57

A΄ Prescribed Performance 59

B′ Dynamical Systems 61

Bibliography 68

List of Figures

1.1 1-dimensional platoon. 10

1.2 Vehicular platoons moving in 2-D. 11

2.1 Graphical illustration of two consecutive vehicles of the platoon. The desired position of the i-th vehicle with respect to its predecessor is denoted by $p_i^* = p_{i-1} - \Delta_{i-1,i}$. Furthermore, each vehicle should keep its distance to the preceding one within the feasible area $\Delta_{\text{col}} < p_{i-1}(t) - p_i(t) < \Delta_{\text{con}}$, thus avoiding collisions and connectivity breaks. 14

2.2 A platoon of N vehicles following a leading vehicle in 1-D Euclidean space. 15

2.3 A typical nonholonomic mobile robot. 16

2.4 Graphical illustration of two consecutive vehicles of the platoon. Each vehicle should its distance $d_i(t)$ and bearing angle $\beta_i(t)$ to its predecessor within the feasible area $d_{\text{col}} < d_i(t) < d_{\text{con}}$ and $|\beta_i(t)| < \beta_{\text{con}}$, thus avoiding collisions and connectivity breaks. 17

3.1 The position of the platoon vehicles. 28

3.2 The evolution of the neighborhood errors $e_{p_i}(t)$, $i = 1, \ldots, 10$ (blue lines) along with the imposed performance bounds (red lines) under the predecessor-following architecture. 28

3.3 The evolution of the neighborhood errors $e_{p_i}(t)$, $i = 1, \ldots, 10$ (blue lines) along with the imposed performance bounds (red lines) under the bidirectional architecture. 29

3.4 The required control input signals under the pred. following architecture. 30

3.5 The required control input signals under the bidirectional architecture. . 30

3.6 The distance between successive vehicles along with the collision and connectivity constraints under the predecessor-following architecture for $N = 10$ vehicles. 31

3.7 The distance between successive vehicles along with the collision and connectivity constraints under the bidirectional architecture for $N = 10$ vehicles. 31

3.8 The distance between successive vehicles along with the collision and connectivity constraints under the predecessor-following architecture for $N = 30$ vehicles. 32

3.9 The distance between successive vehicles along with the collision and connectivity constraints under the predecessor-following architecture for $N = 100$ vehicles. 32
3.10 Comparison of E under the predecessor-following architecture. 33
3.11 Comparison of E under the bidirectional architecture. 33
3.12 Intial pose of the platoon vehicles in the WEBOTS^{TM} simulation. 42
3.13 The trajectories on a planar surface of the vehicles composing the platoon. 43
3.14 The evolution of the distance errors $e_{d_i}(t), i = 1, \ldots, 7$ (blue lines), along with the imposed performance bounds (red lines). 44
3.15 The evolution of the heading errors $e_{\beta_i}(t), i = 1, \ldots, 7$ (blue lines), along with the imposed performance boundes (red lines). 45
3.16 The distance between successive vehicles along with the collision and connectivity constraints. 45
3.17 The orientation angle of each vehicle. 46
3.18 Snapshot of the 2-D vehicle platoon simulation in WEBOTS^{TM}. 46
3.19 Snapshot of the 2-D vehicle platoon simulation in WEBOTS^{TM}. 47

4.1 A Pioneer 2AT mobile robot. 49
4.2 A KUKA Youbot. 50
4.3 A Pioneer 2DX mobile robot. 50
4.4 The position of the platoon vehicles of the experiment. 51
4.5 The evolution of the distance errors $e_{p_i}(t), i = 1, \ldots, 4$ (blue lines), along with the imposed performance bounds (red lines) for the experiment. . . 52
4.6 The required control input signals for the experiment. 52
4.7 The distance between successive vehicles along with the collision and connectivity constraints for the experiment. 53

A′.1 Graphical illustration of the prescribed performance definition 60

Chapter 1

Introduction

1.1 Purpose

The purpose of this work is to propose a decentralized control protocol for vehicular platoons moving in 1-dimensional and 2-dimensional Euclidean space. In particular, we design a control scheme for the 1-D case under two architectures, the predecessor-following, where each vehicle utilizes relative information with respect to its preceding vehicle, and the bidirectional architecture, where each vehicle takes into account relative information from its follower vehicle as well. In that sense, the proposed control protocol is fully decentralized, since the control signal of each agent is calculated based solely on local relative information from its on-board sensors. Furthermore, we propose a decentralized control protocol for vehicular platoons moving in 2-D, where each vehicle has access only to the relative distance and heading error with respect to its preceding vehicle through a mounted camera. Both control protocols create arbitrarily fast and maintain with arbitrary accuracy a desired feasible formation without any intervehicular collisions and connecttivity breaks (owing to limited sensing capabilities). More specifically, each agent in the 1-D case aims at keeping a prespecified desired distance from its neighboring vehicles, whereas in the 2-D case each agent aims at keeping a prespecified desired distance from its preceding vehicle, while keeping it in the field of view of its onboard camera in order to maintain visual connectivity. In addition, the proposed schemes do not require any prior knowledge of the vehicles' dynamic model or external disturbances and no estimation models are employed to acquire such knowledge. Moreover, the transient and steady state response is fully decoupled by the number of vehicles composing the platoon, the control gains selection and the vehicles' model uncertainties. In particular, the achieved performance as well as the collision avoidance and the connectivity maintenance are a priori and explicitly imposed by certain designer-specified performance functions that incorporate the aforementioned sensing capabilities. Finally, the complexity of the overall control architecture proves to be considerably low, since very few and simple calculations are required to output the control signal. In summary, in this work:

- We propose a novel solution to 1-D and 2-D formation problem of vehicular platoons with unknown nonlinear dynamics, avoiding collisions and connectivity breaks owing

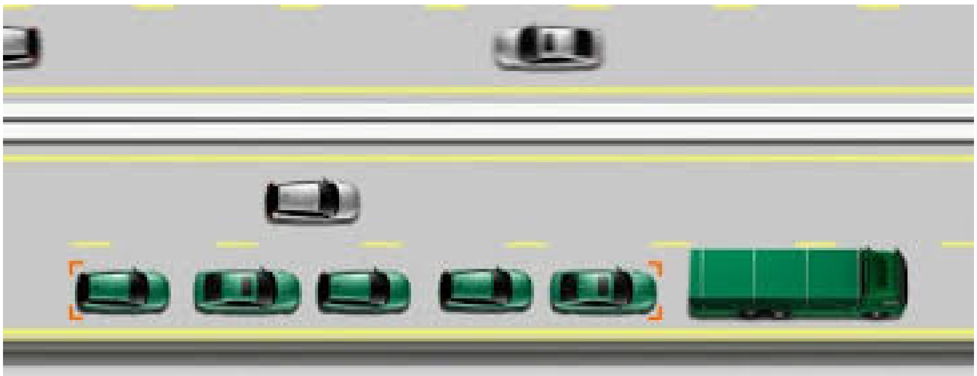

Fig. 1.1: *1-dimensional platoon.*

to feedback constraints imposed by the sensors and the cameras.

- We develop a fully decentralized control protocol, in the sense that the feedback of each vehicle is based exclusively on local information with respect to neighboring vehicles, without incorporating any measurement of the velocity of other vehicles.
- The transient and steady state response of the closed loop system is explicitly determined by certain designer specified performance functions, simplifying thus the control gain selection.

1.2 Bibliography Review

During the last few decades the Automated Highway Systems (AHS) have drawn a notable amount of attention in the field of automatic control. Unlike human drivers that are not able to react quickly and accurately enough to follow each other in close proximity at high speeds, the safety and capacity of highways (measured in vehicles/lanes/time) is significantly increased when vehicles operate autonomously forming large platoons at close spacing. Guaranteed string stability [1] was first achieved via centralized control schemes [2, 1, 3, 4, 5, 6, 7, 8, 9, 10, 11, 12, 13, 14, 15, 16], with all vehicles either communicating explicitly with each other or sending information to a central computer that determines the control protocol. To enhance the overall system's autonomy and avoid delay problems due to wireless communication (as examined in [14]), decentralized schemes were developed, dealing either with the predecessor-following architecture [17, 18, 19, 20, 21, 22, 23, 24, 25, 26, 27, 28], where each vehicle has access to its relative position with respect to its preceding vehicle, or the bidirectional architecture [29, 30, 31, 32, 33, 34, 35, 36], where each vehicle measures its relative position with respect to its following vehicle as well. Finally, in a few works [37, 38, 39] a combined predecessor and leader-following architecture was developed according to which each vehicle obtains additional information from the leading vehicle. The majority of the works in the related literature either considers linear vehicle dynamic models and controllers [3, 4, 18, 26, 27, 32, 40, 41, 42] or adopt linearization techniques and/or Linear Quadratic

Fig. 1.2: *Vehicular platoons moving in 2-D.*

optimal control [29, 20, 22, 23, 25, 38, 43, 44, 45, 46]. However, linearization may lead to unstable inner dynamics since the estimated linear models deviate in general from the real ones, away from the corresponding linearization points. In particular, a comparison of the aforementioned control architectures was carried out in [41], where it was stated that double integrator models with linear controllers and predecessor-following architecture may lead to string instability due to disturbances. In [47] a comparison of two common techniques was conducted, namely the constant time headway policy [21, 22, 25] and the constant spacing policy [31, 41], that are related to the inter-vehicular distances of the platoon. For the latter technique particularly, it is also stated that feedback from the leader vehicle needs to be constantly broadcasted.

The extension of the aforementioned studies to the 2-dimensional case (i.e., when a platoon of vehicles moves in 2-D Euclidean space) is crucial, since realistic situations necessitate for 2-D motion on planar surfaces (see Fig. 1.2). Early works in [11, 48, 9, 6] consider the lane-keeping and lane-changing control for platoons in AHS, adopting however a centralized network, where all vehicles exchange information with a central computer that determines the control protocol, making thus the overall system sensitive to delays, especially when a large number of vehicles is involved. ALternatively, rigid multi-agent formations are employed in decentralized control schemes, where each vehicle utilizes relative information from its neighbors. The majority of these works consider unicycle [49, 50, 51, 52, 53] and bicycle kinematic models [54, 55, 45]. However, many of them adopt linearization techniques [50, 52, 54, 45, 56, 57, 58, 23] that may lead to unstable inner dynamics or degenerate configurations owing to the nonholonomic constraints of the vehicles, as shown in [59].

Additionally, each vehicle is assumed to have access to the neighboring vehicles' velocity, either explicitly, hence degenerating the decentralized manner of the system and imposing inherent communication delays, or by employing observers [53] that increase the overall design complexity. Furthermore, the transient and steady state response of the closed loop is affected severely by the control gains' selection [60], thus limiting the controller's robustness and complicating the control design procedure.

Another significant issue affecting the 2-D control of vehicular platoons concerns the sensing capabilities when visual feedback from camera is adopted. A vast number of the related works neglects the sensory limitations, which however are crucial in real-time scenarios. In [52, 59] visual feedback from omnidirectional cameras is adopted, not accounting thus for sensor limitations, which however are examined in [49] considering directional sensors for the tracking problem of a moving object by a group of robots. Although cameras are directional sensors, they inherently have a limited range and a limited angle of view as well. Hence, in such cases each agent should keep a certain close distance and heading angle from its neighbors, in order to avoid connectivity breaks. Thus, it is clear that limited sensory capabilities lead to additional constraints on the behavior of the system, that should therefore be taken into account exclusively when designing the control protocols. The aforementioned specifications were considered in [61], where a solution based on set-theory and dipolar vector fields was introduced. Alternatively, a visual-servoing scheme for leader-follower formation was presented in [62]. Finally, a centralized control protocol under vision-based localization for leader-follower formations was adopted in [63, 64].

1.3 Structure

The manuscript is organized as follows: The problem statement is given in Chap. 2. Chap. 3 provides the control protocol and extensive simulations results for both the 1-D and 2-D case are also presented. An experimental evaluation for the 1-dimensional case is carried out in Chap. 4. Finally, we conclude in Chap. 5.

Chapter 2

Problem Statement

2.1 1-Dimensional Case

We consider the formation control problem of N vehicles moving in 1-D Euclidean space with 2nd order nonlinear dynamics:

$$\left.\begin{aligned} \dot{p}_i &= v_i \\ m_i\dot{v}_i &= f_i(v_i) + u_i + w_i(t) \end{aligned}\right\}, \ i = 1, \ldots, N \tag{2.1}$$

where $\dot{p}_i$ and v_i denote the position and velocity of each vehicle respectively, m_i is the mass, which is considered unknown, $f_i(v_i)$ is an unknown continuous nonlinear function, u_i is the control input and $w_i(t)$ is a bounded piecewise continuous function of time representing exogenous disturbances. The control objective is to design a distributed control protocol such that a rigid formation is established with prescribed transient and steady state performance, despite the presence of model uncertainties. By prescribed performance, we mean that the formation is achieved in a predefined transient period and is maintained arbitrarily accurate while avoiding collisions and connectivity breaks with neighboring vehicles. The geometry of the formation is represented by the desired gaps $\Delta_{i-1,i}$, $i = 1, \ldots, N$ between two consecutive vehicles (see Fig. 2.1), where $\Delta_{i-1,i} > 0$ denotes the desired distance between the $(i-1)$-th and i-th vehicle (i.e., $p_i(t) \to p_{i-1}(t) - \Delta_{i-1,i}$). Moreover, the distance $p_{i-1}(t) - p_i(t)$ should be kept greater than Δ_{col} to avoid collisions and less than Δ_{con} to maintain the network connectivity owing to the limited sensing capabilities of the vehicles (e.g., when employing range finders to measure the distance between two successive vehicles). Furthermore, to ensure the feasibility of the desired formation, we assume that $\Delta_{\text{col}} < \Delta_{i-1,i} < \Delta_{\text{con}}$, $i = 1, \ldots, N$. Additionally, the desired trajectory of the formation is generated by a reference/leading vehicle denoted by $p_0(t)$ with bounded velocity $v_0(t)$ and is only provided to the first vehicle. Finally, to solve the aforementioned formation control problem, the following assumption is required.

Assumption A1. The initial state of the platoon does not violate the collision and connectivity constraints. That is $\Delta_{\text{col}} < p_{i-1}(0) - p_i(0) < \Delta_{\text{con}}$, $i = 1, \ldots, N$.

In this work, we consider two decentralized control architectures: the predecessor-

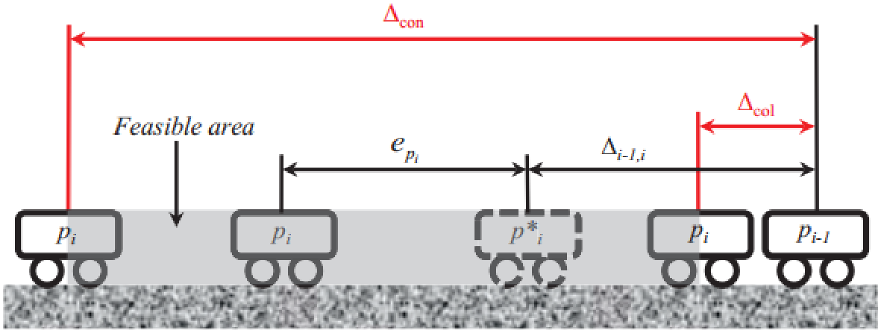

Fig. 2.1: *Graphical illustration of two consecutive vehicles of the platoon. The desired position of the i-th vehicle with respect to its predecessor is denoted by* $p_i^* = p_{i-1} - \Delta_{i-1,i}$*. Furthermore, each vehicle should keep its distance to the preceding one within the feasible area* $\Delta_{\text{col}} < p_{i-1}(t) - p_i(t) < \Delta_{\text{con}}$*, thus avoiding collisions and connectivity breaks.*

following, according to which the control action of each vehicle is based only on its preceding vehicle and the bidirectional architecture, where the control action of each vehicle depends equally on the information from both its preceding and its follower vehicle. Hence, let us formulate N control variables as follows:

$$e_{p_i}(t) = p_{i-1}(t) - p_i(t) - \Delta_{i-1,i},\, i = 1, \dots, N.$$

Equivalently, the neighborhood error vector $e_p = [e_{p_1}, \dots, e_{p_N}]^T$ may be expressed with respect to the leading vehicle as follows:

$$e_p = S(\bar{p}_0 - p - \bar{\Delta}_0) \tag{2.2}$$

where $p = [p_1, \dots, p_N]^T \in \Re^n, \bar{p}_0 := [p_0, \dots, p_0]^T \in \Re^n, \bar{\Delta}_0 := [\Delta_{0,1}, \Delta_{0,2}, \dots, \Delta_{0,N}]^T \in \Re^n$ with $\Delta_{0,i} = \sum_{j=1}^{i} \Delta_{j-1,j}$, $i = 1, \dots, N$ and S is the augmented Laplacian of the graph:

$$S = \begin{bmatrix} 1 & 0 & 0 & \dots & & 0 \\ -1 & 1 & 0 & & & \\ 0 & -1 & 1 & \ddots & & \vdots \\ \vdots & & \ddots & \ddots & & 0 \\ & & & -1 & 1 & 0 \\ 0 & & \dots & 0 & -1 & 1 \end{bmatrix} \tag{2.3}$$

which has strictly positive singular values owing to the strong connectivity of the considered directed graph [65]. Moreover, since all principal minors of S equal to 1, S is also a nonsingular M-matrix [66]. Finally, the following technical lemma plays an important role in the subsequent analysis.

Lemma 2.1. *[65] For a nonsingular M-matrix* $A \in \Re^{N \times N}$*, there exists a diagonal positive definite matrix* $P = (diag(A^{-1}\underline{1}))^{-1}$ *such that the matrix* $Q = PA + A^T P$ *is positive definite as well.*

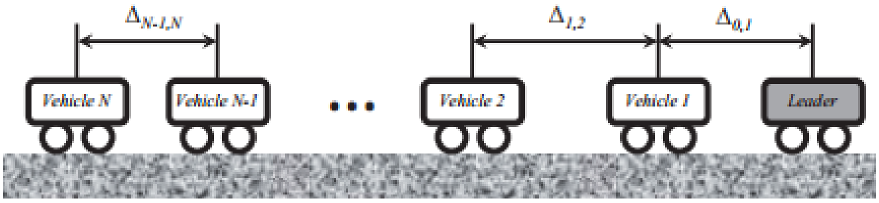

Fig. 2.2: *A platoon of N vehicles following a leading vehicle in 1-D Euclidean space.*

2.2 2-Dimensional Case

Similarly to the 1-Dimensional case, we consider a platoon of N vehicles moving on a planar surface with kinematics:

$$\left.\begin{aligned} \dot{x}_i &= \tfrac{r_i}{2}(\dot{\theta}_{R_i} + \dot{\theta}_{L_i})\cos\phi_i \\ \dot{y}_i &= \tfrac{r_i}{2}(\dot{\theta}_{R_i} + \dot{\theta}_{L_i})\sin\phi_i \\ \dot{\phi}_i &= \tfrac{r_i}{2R_i}(\dot{\theta}_{R_i} - \dot{\theta}_{L_i}) \end{aligned}\right\},\ i = 1,\dots,N \tag{2.4}$$

where x_i, y_i, ϕ_i denote the position and orientation of the center of mass of each vehicle, $\dot{\theta}_{R_i}$ and $\dot{\theta}_{L_i}$ are the angular velocities of the right and left wheel respectively, r_i is the wheel raidus and R_i is the axle length between the wheels (see Fig. 2.3), which are both considered unknown. Let point A denote the center of the axle connecting the two wheels centers. Then its linear and angular velocity are :

$$\left.\begin{aligned} v_{A_i} &= \tfrac{r_i}{2}(\dot{\theta}_{R_i} + \dot{\theta}_{L_i}) \\ \omega_{A_i} &= \tfrac{r_i}{2R_i}(\dot{\theta}_{R_i} - \dot{\theta}_{L_i}) \end{aligned}\right\},\ i = 1,\dots,N. \tag{2.5}$$

Furthermore, following [67], we consider the mobile robot dynamics as follows:

$$M_i\ddot{\vartheta}_i = \tau_i + k_i(\dot{\vartheta}_i) + n_i(t),\ i = 1,\dots,N \tag{2.6}$$

with $\vartheta_i = [\theta_{R_i}\ \theta_{L_i}]^T$ and M_i denoting the positive definite inertia matrix:

$$M_i = \begin{bmatrix} \frac{m_i r_i^2}{4} + \frac{(I_{A_i}+m_i l_i^2)r_i^2}{4R_i^2} + I_{0_i} & \frac{m_i r_i^2}{4} - \frac{(I_{A_i}+m_i l_i^2)r_i^2}{4R_i^2} \\ \frac{m_i r_i^2}{4} - \frac{(I_{A_i}+m_i l_i^2)r_i^2}{4R_i^2} & \frac{m_i r_i^2}{4} + \frac{(I_{A_i}+m_i l_i^2)r_i^2}{4R_i^2} + I_{0_i} \end{bmatrix},\ i = 1,\dots,N \tag{2.7}$$

where m_i is the unknown mass of each vehicle, I_{A_i} is the unknown moment of inertia of the robot about the axis perpendicular to the plane passing from point A and I_{0_i} is the unknown moment of inertia of each wheel about the axle connecting the two wheel centers. Moreover, l_i is the distance from point A to the center of mass along the longitudinal direction of the vehicle (see Fig. 2.3). Finally, $k_i(\dot{\vartheta}_i) : R^2 \to R^2$ are unknown continuous nonlinear functions, $\tau_i = [\tau_{R_i}\ \tau_{L_i}]^T$ are the wheel torques and $n_i(t) : [0,\infty) \to R^2$ are bounded piecewise continuous functions of time representing external

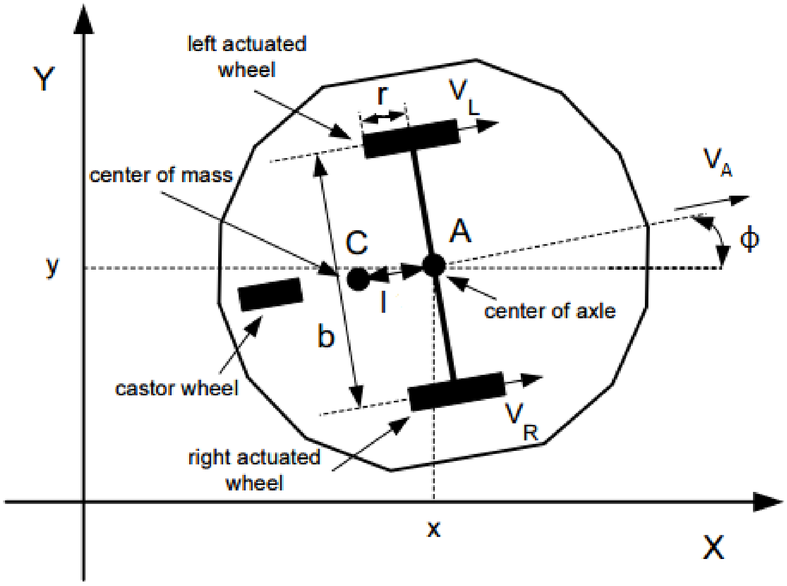

Fig. 2.3: *A typical nonholonomic mobile robot.*

disturbances for $i = 1, \ldots, N$.

In addition, we denote by $d_i(t)$ and $\beta_i(t)$ the distance and the bearing angle between successive vehicles i and $i-1$ (see Fig. 2.4), which we assume are the only available sensor measurements that emanate from an onboard camera that detects a specific marker on the preceding vehicle (e.g. the number plate). The control objective is to design a distributed control protocol based exclusively on visual feedback such that $d_i(t) \to d_{i,des}$ and $\beta_i(t) \to 0$, i.e., each vehicle tracks its predecessor and maintains a prespecified desired distance $d_{i,des}$. Additionally, $d_i(t)$ should be kept greater than d_{col} to avoid collision between successive vehicles. In the same vein, the inter-vehicular distance $d_i(t)$ and the bearing angle $\beta_i(t)$ should be kept less than $d_{\text{con}} > d_{\text{col}}$ and β_{con} respectively, in order to maintain the network connectivity owing to the camera's limited field of view (see Fig. 2.4). Moreover, the desired trajectory of the formation is generated by a reference/leading vehicle:

$$\begin{aligned} \dot{x}_0 &= v_{A_0} \cos\phi_0 \\ \dot{y}_0 &= v_{A_0} \sin\phi_0 \\ \dot{\phi}_0 &= \omega_{A_0} \end{aligned} \tag{2.8}$$

with bounded velocities $v_{A_0}(t)$, $\omega_{A_0}(t)$ and is only provided to the first vehicle. Finally, to solve the aforementioned control problem, we assume that initially each vehicle lies within the field of view of its follower's camera and no collision occurs, wich are rigorously formulated as follows:

Assumption A2. The initial state of the platoon does not violate the collision and connectiviy constraints, i.e., $d_{\text{col}} < d_i(0) < d_{\text{con}}$ and $|\beta_i(0)| < \beta_{\text{con}}$, $i = 1, \ldots, N$.

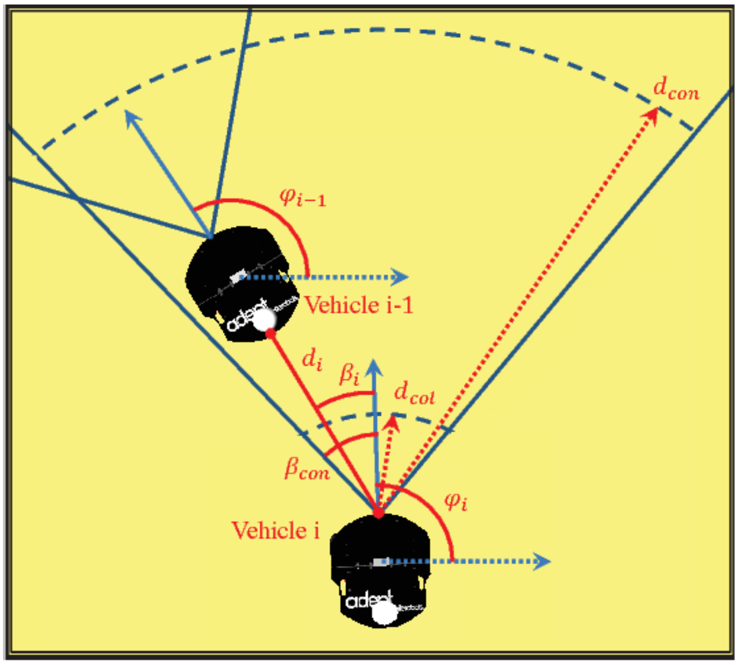

Fig. 2.4: *Graphical illustration of two consecutive vehicles of the platoon. Each vehicle should its distance $d_i(t)$ and bearing angle $\beta_i(t)$ to its predecessor within the feasible area $d_{\text{col}} < d_i(t) < d_{\text{con}}$ and $|\beta_i(t)| < \beta_{\text{con}}$, thus avoiding collisions and connectivity breaks.*

In the sequel, we define the distance and orientation errors:

$$\left.\begin{aligned} e_{d_i}(t) &= d_i(t) - d_{i,des} \\ e_{\beta_i}(t) &= \beta_i(t) \end{aligned}\right\}, \ i = 1, \ldots, N \tag{2.9}$$

where $d_i(t) = \sqrt{(x_i(t) - x_{i-1}(t))^2 + (y_i(t) - y_{i-1}(t))^2}$. Hence, differentiating (2.9) with respect to time and substituting (2.4) and (2.8), we obtain:

$$\left.\begin{aligned} \dot{e}_{d_i}(t) &= -\tfrac{r_i}{2}(\dot{\theta}_{R_i} + \dot{\theta}_{L_i}) \cos\beta_i + \tfrac{r_i}{2}(\dot{\theta}_{R_{i-1}} + \dot{\theta}_{L_{i-1}}) \cos(\gamma_i + \beta_i) \\ \dot{e}_{\beta_i}(t) &= -\tfrac{r_i}{2R}(\dot{\theta}_{R_i} - \dot{\theta}_{L_i}) + \tfrac{r_i}{2d_i}(\dot{\theta}_{R_i} + \dot{\theta}_{L_i}) \sin\beta_i - \tfrac{r_i}{2d_i}(\dot{\theta}_{R_{i-1}} + \dot{\theta}_{L_{i-1}}) \sin(\gamma_i + \beta_i) \end{aligned}\right\}, \ i = 1, \ldots, N \tag{2.10}$$

where $\gamma_i(t) = \phi_i(t) - \phi_{i-1}(t)$ and the following relations have been utilized:

$$\left.\begin{aligned} \cos(\phi_i + \beta_i) &= \tfrac{x_i - x_{i-1}}{d_i} \\ \sin(\phi_i + \beta_i) &= \tfrac{y_i - y_{i-1}}{d_i} \end{aligned}\right\}, \ i = 1, \ldots, N.$$

The error dynamics (2.10) can be expressed in vector form as follows:

$$\begin{aligned} \dot{e}_d &= -\frac{1}{2}\tilde{C}r(\dot{\theta}_R + \dot{\theta}_L) + c \\ \dot{e}_\beta &= -\frac{1}{2}rR^{-1}(\dot{\theta}_R - \dot{\theta}_L) + \frac{1}{2}D^{-1}r[\tilde{S}(\dot{\theta}_R + \dot{\theta}_L) + s] \end{aligned} \tag{2.11}$$

where

$$
\begin{aligned}
e_j &= [e_{j_1}, \dots, e_{j_N}]^T,\ j \in \{d, \beta\} \\
\theta_j &= [\theta_{j_1}, \dots, \theta_{j_N}]^T,\ j \in \{R, L\} \\
r &= diag(r_1, \dots, r_N) \\
D &= diag(d_1, \dots, d_N) \\
R &= diag(R_1, \dots, R_N) \\
c &= [\frac{r_0}{2}(\dot{\theta}_{R_0} + \dot{\theta}_{L_0}) \cos(\gamma_1 + \beta_1), 0, \dots, 0]^T \\
s &= [\frac{r_0}{2}(\dot{\theta}_{R_0} + \dot{\theta}_{L_0}) \sin(\gamma_1 + \beta_1), 0, \dots, 0]^T
\end{aligned}
$$

and $\tilde{C}$, $\tilde{S}$ are the following bidiagonal matrices:

$$
\tilde{C} = \begin{bmatrix}
\cos\beta_1 & 0 & \cdots & 0 \\
-\cos(\gamma_2 + \beta_2) & \cos\beta_2 & & \vdots \\
0 & \ddots & \ddots & \\
 & & \ddots & 0 \\
0 & \cdots & -\cos(\gamma_N + \beta_N) & \cos\beta_N
\end{bmatrix}
$$

$$
\tilde{S} = \begin{bmatrix}
\sin\beta_1 & 0 & \cdots & 0 \\
-\sin(\gamma_2 + \beta_2) & \sin\beta_2 & & \vdots \\
0 & \ddots & \ddots & \\
 & & \ddots & 0 \\
0 & \cdots & -\sin(\gamma_N + \beta_N) & \sin\beta_N
\end{bmatrix}
$$

Chapter 3

Main Results

3.1 1-Dimensional Case

In this work, prescribed performance control, which was recently proposed in [68], will be adopted in order: i) to achieve predefined transient and steady state response for each neighborhood position error $e_{p_i}(t)$, $i = 1, \ldots, N$ as well as ii) to avoid the violation of the collision and connectivity constraints as presented in Section 2.1. Following Appendix A′, prescribed performance is achieved when the neighborhood position errors $e_{p_i}(t), i = 1, \ldots, N$ evolve strictly within a predefined region that is bounded by absolutely decaying functions of time, called performance functions. The mathematical expression of prescribed performance is given by the following inequalities:

$$-\underline{M}_{p_i}\rho_{p_i}(t) < e_{p_i}(t) < \overline{M}_{p_i}\rho_{p_i}(t), \forall t \geq 0 \tag{3.1}$$

for all $i = 1, \ldots, N$, where:

$$\rho_{p_i}(t) = (1 - \frac{\rho_\infty}{\max\{\underline{M}_{p_i}, \overline{M}_{p_i}\}})e^{-lt} + \frac{\rho_\infty}{\max\{\underline{M}_{p_i}, \overline{M}_{p_i}\}} \tag{3.2}$$

are designer-specified, smooth, bounded and decreasing functions of time with l, ρ_∞ positive parameters incorporating the desired transient and steady state performance specifications respectively, and $\underline{M}_{p_i}, \overline{M}_{p_i}, i = 1, \ldots, N$ positive parameters selected appropriately to satisfy the collision and connectivity constraints, as presented in the sequel. In particular, the decreasing rate of $\rho_{p_i}(t), i = 1, \ldots, N$ which is affected by the constant l, introduces a lower bound on the speed of convergence of $e_{p_i}(t)$, $i = 1, \ldots, N$. Furthermore, the constant ρ_∞ can be set arbitrarily small, thus achieving practical convergence of $e_{p_i}(t)$, $i = 1, \ldots, N$ to zero. Additionally, we select:

$$\left.\begin{aligned} \underline{M}_{p_i} &= \Delta_{i-1,i} - \Delta_{\text{col}} \\ \overline{M}_{p_i} &= \Delta_{\text{con}} - \Delta_{i-1,i} \end{aligned}\right\} i = 1, \ldots, N. \tag{3.3}$$

Apparently, since the desired formation is compatible with the collision and connectivity constraints (i.e., $\Delta_{\text{col}} < \Delta_{i-1,i} < \Delta_{\text{con}}$, $i = 1, \ldots, N$), the aforementioned selection ensures that $\underline{M}_{p_i}$, $\overline{M}_{p_i} > 0$, $i = 1, \ldots, N$ and consequently under **Assumption A1** (i.e.,

$\Delta_{\text{col}} < p_{i-1}(0) - p_i(0) < \Delta_{\text{con}}$, $i = 1, \ldots, N$) that:

$$-\underline{M}_{p_i}\rho_{p_i}(0) < e_{p_i}(0) < \overline{M}_{p_i}\rho_{p_i}(0), i = 1, \ldots, N. \tag{3.4}$$

Hence, guaranteeing prescribed performance via (3.1) and employing the decreasing property of $\rho_{p_i}(t)$, $i = 1, \ldots, N$, we obtain:

$$-\underline{M}_{p_i} < e_{p_i}(t) < \overline{M}_{p_i}, \ \forall t \geq 0$$

and consequently, owing to (3.3):

$$\Delta_{\text{col}} < p_{i-1}(t) - p_i(t) < \Delta_{\text{con}}, \ \forall t \geq 0$$

and for all $i = 1, \ldots, N$, which ensures that the collision and connectivity constraints are satisfied for all $t \geq 0$.

In the sequel, we treat seperately the two control architectures (predecessor-following and bidirectional) and propose a distributed control protocol for each one of them that does not incorporate any information on the vehicles' nonlinear model or the external disturbances and guarantees $-\underline{M}_{p_i}\rho_{p_i}(t) < e_{p_i}(t) < \overline{M}_{p_i}\rho_{p_i}(t)$, $i = 1, \ldots, N$ for all $t \geq 0$, thus leading to the solution of the robust formation control problem with prescribed performance under collision and connectivity constraints for the considered platoon of vehicles.

I. Kinematic Controller

Given the neighborhood position errors $e_{p_i}(t) = p_{i-1}(t) - p_i(t) - \Delta_{i-1,i}$, $i = 1, \ldots, N$:

Step I-a. *Select the corresponding functions* $\rho_{p_i}(t)$ *and positive parameters* $\underline{M}_{p_i}$, $\overline{M}_{p_i}$, $i = 1, \ldots, N$ *following (3.2) and (3.3) respectively, in order to incorporate the desired transient and steady state performance specifications as well as the collision and connectivity constraints.*

Step I-b. *Define the normalized neighborhood position errors as:*

$$\xi_p(e_p, t) = \begin{bmatrix} \xi_{p_1}(e_{p_1}, t) \\ \vdots \\ \xi_{p_N}(e_{p_N}, t) \end{bmatrix} := \begin{bmatrix} \frac{e_{p_1}}{\rho_{p_1}(t)} \\ \vdots \\ \frac{e_{p_N}}{\rho_{p_N}(t)} \end{bmatrix} \triangleq (\rho_p(t))^{-1} e_p \tag{3.5}$$

where $\rho_p(t) = diag([\rho_{p_i}(t)]_{i=1,\ldots,N})$ *as well as the expressions:*

$$r_p(\xi_p) = diag([\frac{\frac{1}{\underline{M}_{p_i}} + \frac{1}{\overline{M}_{p_i}}}{(1 + \frac{\xi_{p_i}}{\underline{M}_{p_i}})(1 - \frac{\xi_{p_i}}{\overline{M}_{p_i}})}]_{i=1,\ldots,N}) \tag{3.6}$$

$$\varepsilon_p(\xi_p) = \left[\ln(\frac{1 + \frac{\xi_{p_1}}{\underline{M}_{p_i}}}{1 - \frac{\xi_{p_1}}{\overline{M}_{p_i}}}), \ldots, \ln(\frac{1 + \frac{\xi_{p_N}}{\underline{M}_{p_N}}}{1 - \frac{\xi_{p_N}}{\overline{M}_{p_N}}}) \right]^T \tag{3.7}$$

Step I-c. *Design the decentralized reference velocity vector seperately for the two control architectures as follows:*

A. Predecessor-Following architecture

$$v_d(\xi_p,t)=\begin{bmatrix} v_{d_1}(\xi_{p_1},t)\\ \vdots \\ v_{d_{N-1}}(\xi_{p_{N-1}},t)\\ v_{d_N}(\xi_{p_N},t)\end{bmatrix}=k_p(\rho_p(t))^{-1}r_p(\xi_p)\varepsilon_p(\xi_p) \tag{3.8}$$

B. Bidirectional architecture

$$v_d(\xi_p,t)=\begin{bmatrix} v_{d_1}(\xi_{p_1},\xi_{p_2},t)\\ \vdots \\ v_{d_{N-1}}(\xi_{p_{N-1}},\xi_{p_N},t)\\ v_{d_N}(\xi_{p_N},t)\end{bmatrix}=k_pS^T(\rho_p(t))^{-1}r_p(\xi_p)\varepsilon_p(\xi_p) \tag{3.9}$$

with $k_p>0$ in both cases.

II. Dynamic Controller

Step II-a. *Define the velocity error vector* $e_v=[e_{v_1},\dots,e_{v_N}]^T=v-v_d(\xi_p,t)$ with $v=[v_1,\dots,v_N]^T$ *and select the corresponding velocity performance functions* $\rho_{v_i}(t)$, $i=1,\dots,N$ such that $\rho_{v_i}(0)>|e_{v_i}(0)|$, $i=1,\dots,N$.

Step II-b. *Similarly to the first step define the normalized velocity errors as:*

$$\xi_v(e_v,t)=\begin{bmatrix}\xi_{v_1}(e_{v_1},t)\\ \vdots \\ \xi_{v_N}(e_{v_N},t)\end{bmatrix}:=\begin{bmatrix}\frac{e_{v_1}}{\rho_{v_1}(t)}\\ \vdots \\ \frac{e_{v_N}}{\rho_{v_N}(t)}\end{bmatrix}\triangleq(\rho_v(t))^{-1}e_v \tag{3.10}$$

where $\rho_v(t)=diag([\rho_{v_i}(t)]_{i=1,\dots,N})$ *as well as the expressions:*

$$r_v(\xi_v)=diag([\frac{2}{(1+\xi_{v_i})(1-\xi_{v_i})}]_{i=1,\dots,N}) \tag{3.11}$$

$$\varepsilon_v(\xi_v)=\left[\ln(\frac{1+\xi_{v_i}}{1-\xi_{v_i}}),\dots,\ln(\frac{1+\xi_{v_i}}{1-\xi_{v_i}})\right]^T \tag{3.12}$$

Step II-c. *Design the decentralized control protocol, which is identical for the two architectures:*

$$u(\xi_v,t)=\begin{bmatrix}u_1(\xi_{v_1},t)\\ \vdots \\ u_N(\xi_{v_N},t)\end{bmatrix}=-k_v(\rho_v(t))^{-1}r_v(\xi_v)\varepsilon_v(\xi_v) \tag{3.13}$$

with $k_v>0$.

Remark 1. *Notice by (3.8), (3.9) and (3.13) that the proposed control protocol is decentralized in the sense that each vehicle utilizes only local relative information to calculate its own signal. In particular, the desired vehicle velocity as obtained by (3.8) in the predecessor-following architecture utilizes the relative position with respect only to the preceding vehicle whereas the bidirectional architecture considers the relative position with respect to the following vehicle as well by incorporating the matrix S^T in (3.9). Moreover, the* *proposed control law does not incorporate any prior knowledge of the model nonlinearities/disturbances or even of some corresponding upper/lower bounding functions, relaxing thus significantly the key assumptions made in the related literature. Furthermore, the proposed methodology results in a low complexity design. Notice that no hard calculations (neither analytic nor numerical) are required to output the proposed control signal, thus making its distributed implementation straightforward.*

3.1.1 Stability Analysis

The main results of this section are summarized in the following theorem where it is proven that the aforementioned decentralized control protocol solves the robust formation problem with prescribed performance under collision and connectivity constraints for the considered platoon of vehicles both in the predecessor-following and the bidirectional control architecture.

Theorem 3.1. *Consider a platoon of N vehicles of the form (2.1), following a leader in 1-D and aiming at establishing a formation described by the desired gaps* $\Delta_{i-1,i}$*,* $i = 1, \ldots, N$ *between consecutive vehicles, while satisfying the collision and connectivity constraints represented by* Δ_{col} *and* Δ_{con} *respectively with* $\Delta_{\text{col}} < \Delta_{i-1,i} < \Delta_{\text{con}}$*,* $i = 1, \ldots, N$*. Under* ***Assumption A1****, the decentralized control protocol (3.5)-(3.13) guarantees:*

$$-\underline{M}_{p_i}\rho_{p_i}(t) < e_{p_i}(t) < \overline{M}_{p_i}\rho_{p_i}(t), \, \forall t \geq 0$$

for all $i = 1, \ldots, N$*, as well as boundedness of all closed loop signals.*

Proof. Differentiating (3.5) and (3.10) with respect to time, we obtain:

$$\dot{\xi}_p = (\rho_p(t))^{-1}(\dot{e}_p - \dot{\rho}_p(t)\,\xi_p) \tag{3.14}$$

$$\dot{\xi}_v = (\rho_v(t))^{-1}(\dot{e}_v - \dot{\rho}_v(t)\,\xi_v) \tag{3.15}$$

A. Predecessor-Following architecture

Employing (2.1), (2.2) as well as the fact that $v_i = v_{d_i} + \rho_{v_i}(t)\,\xi_{v_i}$ *and substituting (3.8), (3.13) in (3.14) and (3.15), we arrive at:*

$$\begin{aligned}\dot{\xi}_p &= h_p(t,\xi)\\ &= -k_p(\rho_p(t))^{-1}S(\rho_p(t))^{-1}r_p(\xi_p)\varepsilon_p(\xi_p)\\ &\quad - (\rho_p(t))^{-1}(\dot{\rho}_p(t)\,\xi_p + S(\rho_v(t)\,\xi_v - \dot{\bar{p}}_0(t)))\end{aligned} \tag{3.16}$$

$$\begin{aligned}\dot{\xi}_v &= h_v(t,\xi)\\ &= -k_v(\rho_v(t))^{-1}M^{-1}\varepsilon_v(\xi_v) - (\rho_v(t))^{-1}(\dot{\rho}_v(t)\,\xi_v\\ &\quad - M^{-1}(f(v_d + \rho_v(t)\,\xi_v) + w(t)) + \dot{v}_d)\end{aligned} \tag{3.17}$$

where

$$M = diag([m_i]_{i=1,\dots,N})$$
$$f(v_d + \rho_v(t)\,\xi_v) = \begin{bmatrix} f_1(v_{d_1} + \rho_{v_1}(t)\,\xi_{v_1}) \\ \vdots \\ f_N(v_{d_N} + \rho_{v_N}(t)\,\xi_{v_N}) \end{bmatrix}$$

with m_i, $f_i(\cdot)$, $i = 1, \dots, N$ *denoting the unknown mass and nonlinearity of the vehicle model (2.1) respectively. Thus, the closed loop dynamical system of* $\xi(t) = [\xi_p^T(t), \xi_v^T(t)]^T$ *may be written in compact form as:*

$$\dot{\xi} = h(t,\xi) = \begin{bmatrix} h_p(t,\xi) \\ h_v(t,\xi) \end{bmatrix}. \tag{3.18}$$

Let us also define the open set $\Omega_\xi = \Omega_{\xi_p} \times \Omega_{\xi_v} \subset \Re^{2N}$ *with:*

$$\begin{aligned} \Omega_{\xi_p} &= (-\underline{M}_{p_1}, \overline{M}_{p_1}) \times \dots \times (-\underline{M}_{p_N}, \overline{M}_{p_N}) \\ \Omega_{\xi_v} &= \underbrace{(-1,1) \times \dots \times (-1,1)}_{N\text{-times}}. \end{aligned} \tag{3.19}$$

In what follows, we proceed in two phases. First, the existence of a unique maximal solution $\xi(t)$ *of (3.18) over* Ω_ξ *for a time interval* $[0, \tau_{\max})$ *(i.e.,* $\xi(t) \in \Omega_\xi, \forall t \in [0, \tau_{\max})$ *) is ensured. Then, we prove that the proposed control scheme guarantees, for all* $t \in [0, \tau_{\max})$ *: a) the boundedness of all closed loop signals as well as that b)* $\xi(t)$ *remains strictly within a compact subset of* Ω_ξ*, which leads by contradiction to* $\tau_{\max} = \infty$ *and consequently to the completion of the proof.*

Phase A-i. Selecting the parameters $\underline{M}_{p_i}$, $\overline{M}_{p_i}$, $i = 1, \dots, N$ *according to (3.3), we guarantee that the set* Ω_ξ *is nonempty and open. Moreover, as shown in (3.4) owing to* ***Assumption A1****,* $\xi_p(0) \in \Omega_{\xi_p}$*. Furthermore, selecting* $\rho_{v_i}(0) > |e_{v_i}(0)|$, $i = 1, \dots, N$ *we ensure that* $\xi_v(0) \in \Omega_{\xi_v}$ *as well. Thus, we conclude that* $\xi(0) \in \Omega_\xi$*. Additionally, h is continuous on t and locally Lipschitz on* ξ *over the set* Ω_ξ*. Therefore, the hypotheses of Theorem 2.3 stated in Appendix B′ hold and the existence of a maximal solution* $\xi(t)$ *of (3.18) for a time interval* $[0, \tau_{\max})$ *such that* $\xi(t) \in \Omega_\xi, \forall t \in [0, \tau_{\max})$ *is guaranteed.*

Phase A-ii. We have proven in Phase A-i that $\xi(t) \in \Omega_\xi$, $\forall t \in [0, \tau_{\max})$ *and more specifically that:*

$$\left. \begin{aligned} \xi_{p_i} &= \frac{e_{p_i}(t)}{\rho_{p_i}(t)} \in (-\underline{M}_{p_i}, \overline{M}_{p_i}) \\ \xi_{v_i} &= \frac{e_{v_i}(t)}{\rho_{v_i}(t)} \in (-1, 1) \end{aligned} \right\} \; i = 1, \dots, N \tag{3.20}$$

for all $t \in [0, \tau_{\max})$*, from which we obtain that* $e_{p_i}(t)$ *and* $e_{v_i}(t)$ *are absolutely bounded by* $\max\{\underline{M}_{p_i}, \overline{M}_{p_i}\}\rho_{p_i}(t)$ *and* $\rho_{v_i}(t)$ *respectively for* $i = 1, \dots, N$*. Furthermore, owing to (3.20), the error vectors* $\varepsilon_p(t)$ *and* $\varepsilon_v(t)$ *as given in (3.7) and (3.12) are well defined for all* $t \in [0, \tau_{\max})$*. Therefore, consider the positive definite and radially unbounded function* $V_p = \frac{1}{2}\varepsilon_p^T P \varepsilon_p$ *where* $P = (diag(S^{-1}\underline{1}))^{-1}$ *is a diagonal positive definite matrix satisfying* $Q = PS + S^T P > 0$*, as dictated by Lemma 2.1. Differentiating* V_p *with respect to time and* *substituting (3.6), (3.16), we obtain:*

$$\begin{aligned}\dot{V}_p &= -k_p \varepsilon_p^T P r_p(\xi_p)(\rho_p(t))^{-1} S(\rho_p(t))^{-1} r_p(\xi_p)\varepsilon_p(\xi_p)\\ &\quad - \varepsilon_p^T P r_p(\xi_p)(\rho_p(t))^{-1}(\dot{\rho}_p(t)\,\xi_p + S(\rho_v(t)\,\xi_v - \dot{\bar{p}}_0(t))).\end{aligned}$$

Exploiting: i) the diagonality of P, $r_p(\xi_p)$, $\rho_p(t)$ matrices, ii) the positive defineteness of $Q = PS + S^T P$ as well as iii) the boundedness of $\dot{\rho}_p(t)$, $\rho_v(t)$ and $\dot{\bar{p}}_0(t)$, we get:

$$\dot{V}_p \leq -k_p \lambda_{\min}(Q) \left\|\varepsilon_p^T r_p(\xi_p)(\rho_p(t))^{-1}\right\|^2 + \left\|\varepsilon_p^T r_p(\xi_p)(\rho_p(t))^{-1}\right\| \bar{F}_p$$

where F_p is a positive constant indepedent of $\tau_{\max}$, satisfying:

$$\left\|P(\dot{\rho}_p(t)\,\xi_p + S(\rho_v(t)\,\xi_v - \dot{\bar{p}}_0(t)))\right\| \leq \bar{F}_p \tag{3.21}$$

for all $(\xi, t) \in \Omega_\xi \times \Re_+$. Therefore, we conclude that $\dot{V}_p$ is negative when $\left\|\varepsilon_p^T r_p(\xi_p)(\rho_p(t))^{-1}\right\| > \frac{\bar{F}_p}{k_p \lambda_{\min}(Q)}$ from which, owing to the positive definiteness and diagonality of $r_p(\xi_p)(\rho_p(t))^{-1}$ as well as employing (3.6) and (3.2), it can be easily deduced that:

$$\|\varepsilon_p(t)\| \leq \bar{\varepsilon}_p := \max\left\{\varepsilon_p(0), \frac{\bar{F}_p \max\left\{\frac{\underline{M}_{p_i}\overline{M}_{p_i}}{\underline{M}_{p_i}+\overline{M}_{p_i}}\right\}}{k_p \lambda_{\min}(Q)\lambda_{\min}(P)}\right\} \tag{3.22}$$

for all $t \in [0, \tau_{\max})$. Furthermore, from (3.7), taking the inverse logarithm, we obtain:

$$-\underline{M}_{p_i} < \frac{e^{-\bar{\varepsilon}_p} - 1}{e^{-\bar{\varepsilon}_p} + 1}\underline{M}_{p_i} = \underline{\xi}_{p_i} \leq \xi_{p_i}(t) \leq \bar{\xi}_{p_i} = \frac{e^{\bar{\varepsilon}_p} - 1}{e^{\bar{\varepsilon}_p} + 1}\overline{M}_{p_i} < \overline{M}_{p_i} \tag{3.23}$$

for all $t \in [0, \tau_{\max})$ and $i = 1, \ldots, N$. Thus, the reference velocity vector $v_d(\xi_p, t)$, as designed in (3.8), remains bounded for all $t \in [0, \tau_{\max})$. Moreover, invoking $v_i = v_{d_i} + \rho_{v_i}(t)\,\xi_{v_i}$ we also conclude the boundedness of the velocities $v_i(t)$, $i = 1, \ldots, N$ for all $t \in [0, \tau_{\max})$. Finally, differentiating $v_d(\xi_p, t)$ with respect to time, substituting (3.16) and utilizing (3.23), it is straightforward to deduce the boundedness of $\dot{v}_d$ for all $t \in [0, \tau_{\max})$ as well.

B. Bidirectional architecture

Applying the aforementioned line of proof for the bidirectional control architecture as well, we substitute (2.1), (2.2) and (3.9) in (3.14) and invoking $v_i = v_{d_i} + \rho_{v_i}(t)\,\xi_{v_i}$ we get:

$$\begin{aligned}\dot{\xi}_p &= h_{p_2}(t, \xi)\\ &= -k_p(\rho_p(t))^{-1} S S^T (\rho_p(t))^{-1} r_p(\xi_p)\varepsilon_p(\xi_p) \qquad (3.24)\\ &\quad - (\rho_p(t))^{-1}(\dot{\rho}_p(t)\,\xi_p + S(\rho_v(t)\,\xi_v - \dot{\bar{p}}_0(t))). \qquad (3.25)\end{aligned}$$

The closed loop dynamical system is now written as:

$$\dot{\xi} = h_2(t, \xi) = \begin{bmatrix} h_{p_2}(t, \xi) \\ h_{v_2}(t, \xi) \end{bmatrix} \tag{3.26}$$

where $h_{v_2}(t, \xi) = h_v(t, \xi)$ *as defined in (3.17).*

Phase B-i. Notice that h_2 *is continuous on* t *and locally Lipschitz on* ξ *over the set* Ω_ξ *introduced by (3.19). Therefore, proceeding in a similar manner as in the predecessor-following case and guaranteeing that* $\xi(0) \in \Omega_\xi$*, it is straightforward that the existence of a maximal solution of (3.26) on a time interval* $[0, \tau_{\max})$ *such that* $\xi(t) \in \Omega_\xi, \forall t \in [0, \tau_{\max})$ *is ensured. Therefore, (3.20) holds for all* $t \in [0, \tau_{\max})$ *and* $e_{p_i}(t)$ *and* $e_{v_i}(t)$ *are absolutely bounded by* $\max\{\underline{M}_{p_i}, \overline{M}_{p_i}\}\rho_{p_i}(t)$ *and* $\rho_{v_i}(t)$ *respectively for* $i = 1, \ldots, N$*.*

Phase B-ii. It follows from Phase B-i that $\varepsilon_p(t)$ *and* $\varepsilon_v(t)$ *are well defined for all* $t \in [0, \tau_{\max})$ *and thus we consider the positive definite and radially unbounded function* $V_{p_2} = \frac{1}{2}\varepsilon_p^T\varepsilon_p$*. Differentianting* V_{p_2} *with respect to time and substituting (3.6) and (3.24), we obtain:*

$$\begin{aligned}\dot{V}_{p_2} = &-k_p\varepsilon_p^T r_p(\xi_p)(\rho_p\,(t))^{-1}SS^T(\rho_p\,(t))^{-1}r_p(\xi_p)\varepsilon_p(\xi_p)\\ &-\varepsilon_p^T r_p(\xi_p)(\rho_p\,(t))^{-1}(\dot{\rho}_p\,(t)\,\xi_p + S(\rho_v\,(t)\,\xi_v - \dot{\bar{p}}_0(t))).\end{aligned}$$

It can also be easily deduced from (2.3) that:

$$SS^T = \begin{bmatrix} 2 & -1 & 0 & \cdots & & 0\\ -1 & 2 & -1 & & & \\ 0 & -1 & 2 & \ddots & & \vdots\\ \vdots & & \ddots & \ddots & -1 & 0\\ & & & -1 & 2 & -1\\ 0 & & \cdots & 0 & -1 & 1 \end{bmatrix}$$

which is a positive definite matrix satisfying $\lambda_{\min}(SS^T) = 4\sin^2(\frac{\pi}{4N+2})$ *with* N *denoting the number of platoon's vehicles (see Theorem 3.1 in [69]). Thus, exploiting: i) the positive definiteness of* SS^T *as well as ii) the boundedness of* $\dot{\rho}_p\,(t)$*,* $\rho_v\,(t)$ *and* $\dot{\bar{p}}_0(t)$*, we get:*

$$\dot{V}_{p_2} \leq -4k_p\sin^2(\frac{\pi}{4N+2})\left\|\varepsilon_p^T r_p(\xi_p)(\rho_p\,(t))^{-1}\right\|^2 + \left\|\varepsilon_p^T r_p(\xi_p)(\rho_p\,(t))^{-1}\right\|\bar{G}_p$$

where $\bar{G}_p$ *is a positive constant independent of* $\tau_{\max}$*, satisfying:*

$$\left\|\dot{\rho}_p\,(t)\,\xi_p + S(\rho_v\,(t)\,\xi_v - \dot{\bar{p}}_0(t))\right\| \leq \bar{G}_p \tag{3.27}$$

for all $(\xi, t) \in \Omega_\xi \times \Re_+$*. Therefore, we conclude that* $\dot{V}_{p_2}$ *is negative when* $\left\|\varepsilon_p^T r_p(\xi_p)(\rho_p\,(t))^{-1}\right\| > \frac{\bar{G}_p}{4k_p\sin^2(\frac{\pi}{4N+2})}$ *from which, owing to the positive definiteness and diagonality of* $r_p(\xi_p)(\rho_p\,(t))^{-1}$ *as well as employing (3.6) and (3.2), it can be easily verified that:*

$$\|\varepsilon_p(t)\| \leq \bar{\varepsilon}_p := \max\left\{\varepsilon_p(0), \frac{\bar{G}_p\max\left\{\frac{\underline{M}_{p_i}\overline{M}_{p_i}}{\underline{M}_{p_i}+\overline{M}_{p_i}}\right\}}{4k_p\sin^2(\frac{\pi}{4N+2})}\right\} \tag{3.28}$$

for all $t \in [0, \tau_{\max})$*. Therefore, (3.23) holds for all* $t \in [0, \tau_{\max})$ *and* $i = 1, \ldots, N$*. Thus, the* *reference velocity vector $v_d(\xi_p, t)$, as designed in (3.9) for the bidirectional architecture, remains bounded for all $t \in [0, \tau_{\max})$ from which we also conclude the boundedness of $v_i(t), i = 1, \ldots, N$ and $\dot{v}_d$ for all $t \in [0, \tau_{\max})$.*

Regarding the transformed error ε_v and the control signal u, we consider the positive definite and radially unbounded function $V_v = \frac{1}{2}\varepsilon_v^T M \varepsilon_v$ where $M = diag([m_i]_{i=1,\ldots,N})$ with m_i, $i = 1, \ldots, N$ denoting the unknown mass of the vehicle model (2.1), and by following similar analysis with $V_p = \frac{1}{2}\varepsilon_p^T P \varepsilon_p$, we conclude that:

$$\|\varepsilon_v(t)\| \leq \bar{\varepsilon}_v := \max\left\{\varepsilon_v(0), \frac{\bar{F}_v}{2k_v \min\{m_i\}}\right\} \tag{3.29}$$

for all $t \in [0, \tau_{\max})$, where $\bar{F}_v$ is a positive constant satisfying:

$$\|(M\dot{\rho}_v(t)\,\xi_v - (f(v_d + \rho_v(t)\,\xi_v) + w(t)) + \dot{v}_d)\| \leq \bar{F}_v \tag{3.30}$$

owing to: i) the boundedness of v_d and $\dot{v}_d$ that was proven previously, ii) the continuity of function $f_i(\cdot)$ and iii) the boundedness of $\dot{\rho}_v(t)$, $\rho_v(t)$ as well as of the disturbance term $w(t)$. Furthermore, from (3.12), taking the inverse logarithmic function, we obtain:

$$-1 < \frac{e^{-\bar{\varepsilon}_v} - 1}{e^{-\bar{\varepsilon}_v} + 1} = \underline{\xi}_{v_i} \leq \xi_{v_i}(t) \leq \bar{\xi}_{v_i} = \frac{e^{\bar{\varepsilon}_v} - 1}{e^{\bar{\varepsilon}_v} + 1} < 1 \tag{3.31}$$

for all $t \in [0, \tau_{\max})$ and $i = 1, \ldots, N$, which also leads to boundedness of the distributed control protocol (3.13).

Up to this point, we have proven that $\xi(t) \in \Omega_\xi$ as well as the boundedness of all closed signals for all $t \in [0, \tau_{\max})$ both for the predecessor-following and the bidirectional architecture. What remains to be shown is that $\tau_{\max}$ can be extended to ∞. In this direction, notice by (3.23) and (3.31) that $\xi(t) \in \Omega'_\xi = \Omega'_{\xi_p} \times \Omega'_{\xi_v}$, $\forall t \in [0, \tau_{\max})$, where:

$$\Omega'_{\xi_p} = [\underline{\xi}_{p_1}, \bar{\xi}_{p_1}] \times \ldots \times [\underline{\xi}_{p_N}, \bar{\xi}_{p_N}]$$
$$\Omega'_{\xi_v} = [\underline{\xi}_{v_1}, \bar{\xi}_{v_1}] \times \ldots \times [\underline{\xi}_{v_N}, \bar{\xi}_{v_N}]$$

are nonempty and compact subset of Ω_{ξ_p} and Ω_{ξ_v} respectively. Hence, assuming $\tau_{\max} < \infty$ and since $\Omega'_\xi \subset \Omega_\xi$, Proposition 2.1 in Appendix B′ dictates the existence of a time instant $t' \in [0, \tau_{\max})$ such that $\xi(t') \notin \Omega'_\xi$, which is a clear contradiction. Therefore, $\tau_{\max} = \infty$. Thus, all closed loop signals remain bounded and moreover $\xi(t) \in \Omega'_\xi \subset \Omega_\xi$, $\forall t \geq 0$. Finally, multiplying (3.23) by $\rho_{p_i}(t)$, $i = 1, \ldots, N$, we also conclude that:

$$-\underline{M}_{p_i}\rho_{p_i}(t) < e_{p_i}(t) < \overline{M}_{p_i}\rho_{p_i}(t) \tag{3.32}$$

for all $i = 1, \ldots, N$ as well as $t \geq 0$ and consequently the solution of the robust formation control problem with prescribed performance under collision and connectivity constraints for the considered platoon of vehicles.

Remark 2. *From the aforementioned proof it can be deduced that the proposed control scheme achieves its goals withour resorting to the need of rendering $\bar{\varepsilon}_p$, $\bar{\varepsilon}_v$ arbitrarily* *small by adopting extreme values of the control gains k_p and k_v neither in the predecessor-following nor in the biridectional architecture (see (3.22), (3.28) and (3.29)). More specifically, notice that (3.23) and (3.31) hold no matter how large the finite bounds $\bar{\varepsilon}_p$, $\bar{\varepsilon}_v$ are. In the same spirit, large model uncertainties, such as the vehicle masses m_i, $i = 1, \ldots, N$ that are highly dependant on the number of passengers in real-time scenario vehicle platoons, can be compensated, as they affect only the size of $\bar{\varepsilon}_v$ through $\bar{F}_v$ (see (3.30)), but leave unaltered the achieved stability properties. Hence, the actual performance given in (3.32), which is solely determined by the designer-specified funcitons $\rho_{p_i}(t)$ and the parameters $-\underline{M}_{p_i}$, $\overline{M}_{p_i}$, $i = 1, \ldots, N$, becomes isolated against model uncertainties, thus extending greatly the robustness of the proposed control scheme. Furthermore, the selection of the control gains k_p and k_v is significantly simplified to adopting those values that lead to reasonable control effort. Nonetheless, it should be noted that their selection affects the control input characteristics (i.e., decreasing the gain values leads to increased oscillatory behaviour within the prescribed performance envelope described by (3.1), which is improved when adopting higher values, enlarging, however, the control effort both in magnitude and rate). Additionally, fine tuning might be needed in real-time scenarios, to retain the required linear velocity within the range of velocities that can be implemented by the motors. Similarly, the control input constraints impose an upper bound on the required speed of convergence of $\rho_{p_i}(t)$, $i = 1, \ldots, N$, as obtained by the exponentials e^{-lt}.*

3.1.2 Simulations

To demonstrate the efficiency of the proposed distributed control protocol, we consider a platoon of $N = 10$ vehicles with the following nonlinear model:

$$\begin{aligned} \dot{p}_i &= v_i \\ 1.2\dot{v}_i &= -0.5v_i - 0.25\,|v_i|\,v_i + u_i + A_i \sin(\omega_i t + \varphi_i) \end{aligned}$$

with A_i, ω_i, φ_i randomly chosen in $[1.0,\ 1.5]$, $[2.0,\ 2.5]$ and $[0,\ 2\pi]$ respectively. The leader node follows a constant velocity model given by $p_0(t) = 1.5t$. Furthermore, the desired distance between consecutive vehicles is equally set at $\Delta_{i-1,i} = \Delta^* = 0.75$m, $i = 1, \ldots, 10$ whereas the collision and connectivity constraints are given by $\Delta_{\text{col}} = 0.05\Delta^*$ and $\Delta_{\text{con}} = 1.95\Delta^*$ respectively. Notice that the aforementioned formation problem under the collision/connectivity constraints is feasible since $\Delta_{\text{col}} < \Delta_{i-1,i} < \Delta_{\text{con}}$, $i = 1, \ldots, 10$. Moreover, we also require steady state errors of no more than 0.05m and minimum speed of convergence as obtained by the exponential $e^{-0.5t}$. Thus, according to (3.3), we selected the parameters $\underline{M}_{p_i} = \overline{M}_{p_i} = 0.95\Delta^*$, $i = 1, \ldots, 10$ and the functions $\rho_{p_i}(t) = (1 - \frac{0.05}{0.95\Delta^*})e^{-0.5t} + \frac{0.05}{0.95\Delta^*}$, $i = 1, \ldots, 10$ in order to achieve the desired transient and steady state performance specifications as well as to comply with the collision and connectivity constraints. Finally, we chose $\rho_{v_i}(t) = 2\,|e_{v_i}(0)|\,e^{-0.5t} + 0.1$, $i = 1, \ldots, 10$. The control gain values were chosen as $k_p = k_v = 0.25$ for the predecessor-following architecture and $k_p = 0.1$, $k_v = 100$ for the bidirectional architecture. Fig. 3.1 pictures the position of the vehicles with respect to time, which is similar for both cases.

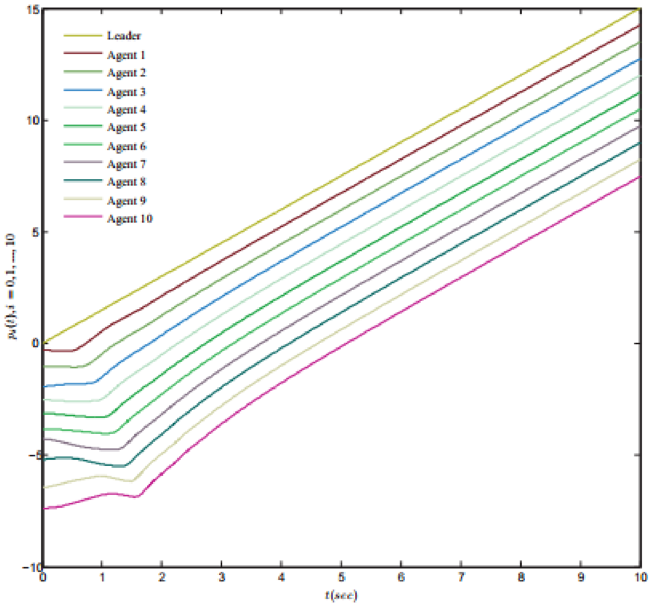

Fig. 3.1: *The position of the platoon vehicles.*

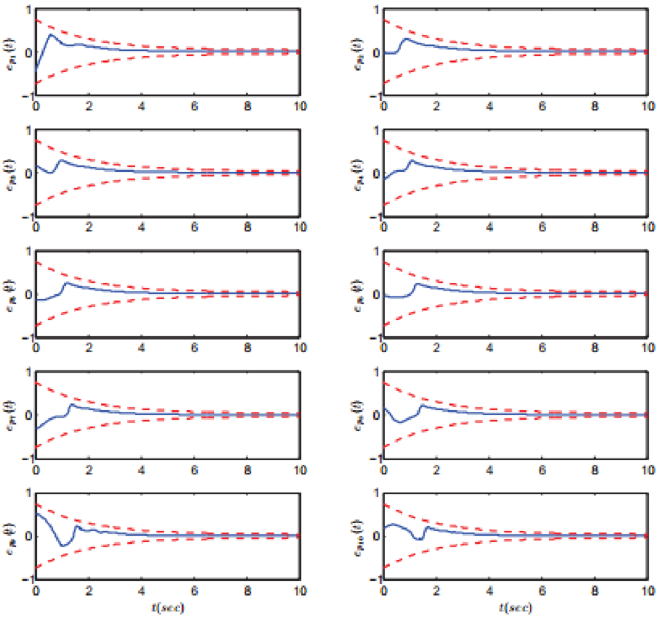

Fig. 3.2: *The evolution of the neighborhood errors* $e_{p_i}(t)$, $i = 1, \ldots, 10$ *(blue lines) along with the imposed performance bounds (red lines) under the predecessor-following architecture.*

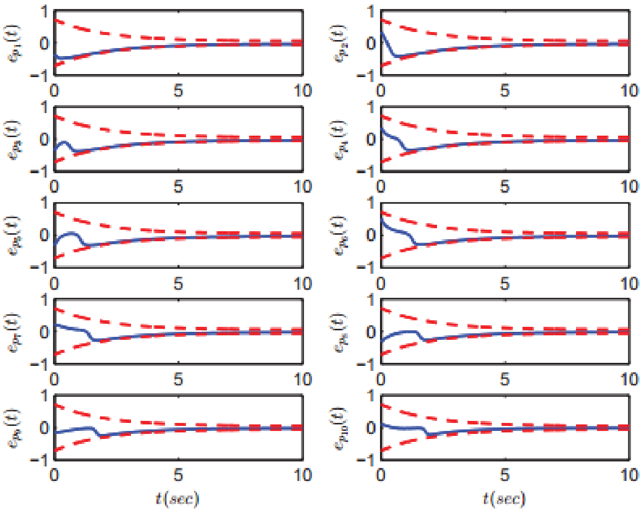

Fig. 3.3: *The evolution of the neighborhood errors $e_{p_i}(t)$, $i = 1, \ldots, 10$ (blue lines) along with the imposed performance bounds (red lines) under the bidirectional architecture.*

The simulation results are illustrated in Figs. 3.2-3.9 for the two different control architectures. More specifically, the evolution of the neighborhood errors $e_{p_i}(t)$, $i = 1, \ldots, 10$ along with the imposed performance bounds by the corresponding performance functions are given in Figs. 3.2 and 3.3, while the required control inputs are illustrated in Figs. 3.4 and 3.5 respectively. Furthermore, Figs. 3.6 and 3.7 depict the intevehicular distances along with the collision and connectivity constraints. The same results for the case of $N = 30$ and $N = 100$ vehicles under the bidirectional control architecture are also given in Figs. 3.8 and 3.9, to verify the robustness of the proposed control protocol against the number of vehicles composing the platoon. It can be easily deduced that guaranteed transient and steady state response as well as collision avoidance and connectivity maintenance are achieved with bounded closed loop signals, despite the presence of external disturbances as well as the lack of knoweldge of the vehicles' dynamics and irrespectively of the number of vehicles composing the platoon.

To further investigate the performance of the proposed 1-D methodology, a comparative simulation was carried out between the presented control scheme and the one suggested in [29], according to aforementioned nonlinear model. For the convenience of comparison, we define the following as a measure of performance:

$$E = \frac{1}{N} \int_0^T \sum_{i=1}^{N} (e_{p_{0,i}}(t) + \dot{e}_{p_{0,i}}(t)) dt \tag{3.33}$$

We study through numerical simulations how E scales with the number of agents N for $T = 10^2$ seconds. Notice that the method proposed in [29] considers a double integrator model and therefore a feedback linearization technique was included in the control scheme. In order to simulate a realistic scenario, however, the model parameters adopted deviated up to 15% from their actual values. The corresponding control gains were tediously selected through a trial-and-error process to yield satisfying performance.

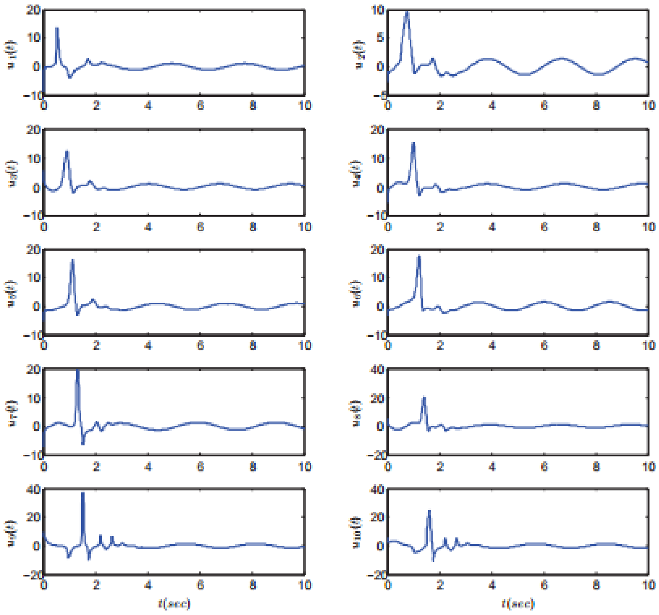

Fig. 3.4: *The required control input signals under the pred. following architecture.*

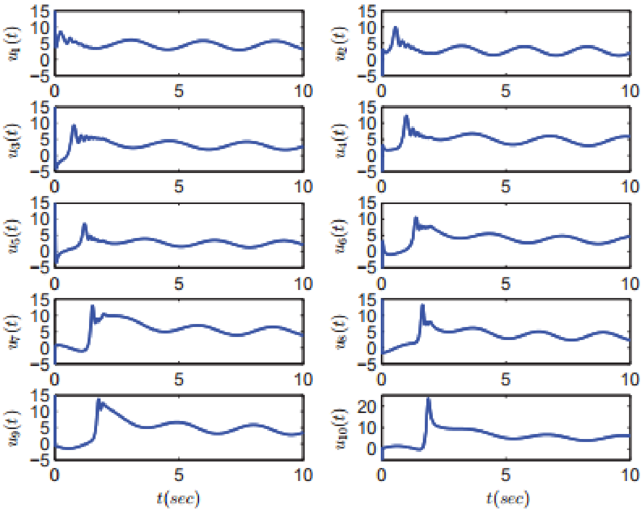

Fig. 3.5: *The required control input signals under the bidirectional architecture.*

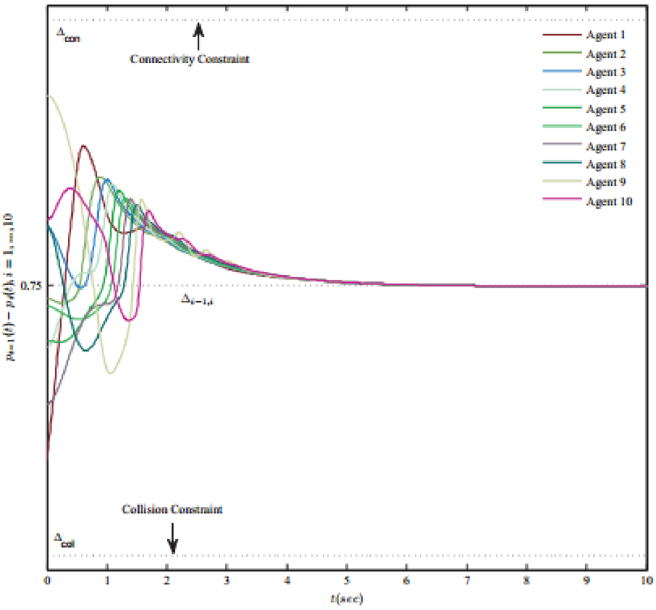

Fig. 3.6: *The distance between successive vehicles along with the collision and connectivity constraints under the predecessor-following architecture for* $N = 10$ *vehicles.*

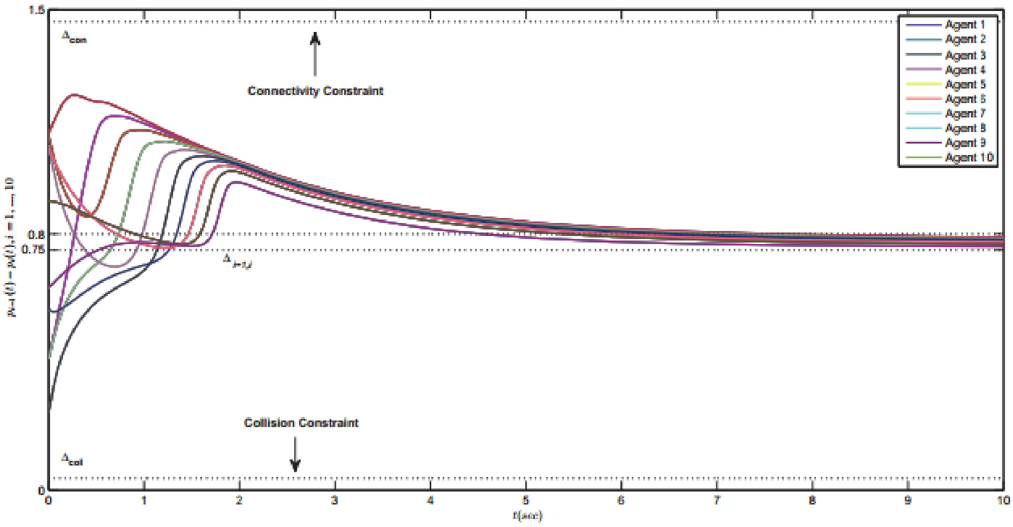

Fig. 3.7: *The distance between successive vehicles along with the collision and connectivity constraints under the bidirectional architecture for* $N = 10$ *vehicles.*

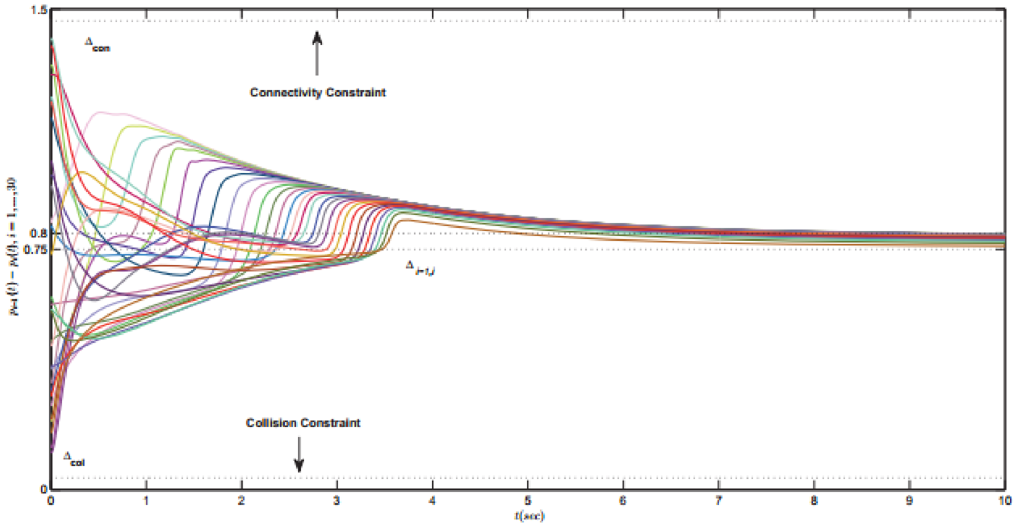

Fig. 3.8: *The distance between successive vehicles along with the collision and connectivity constraints under the predecessor-following architecture for* $N = 30$ *vehicles.*

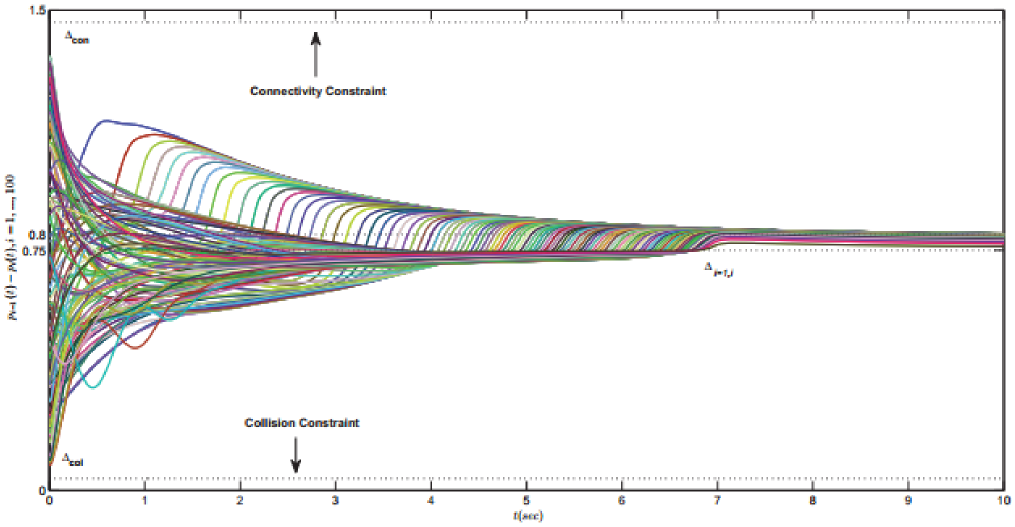

Fig. 3.9: *The distance between successive vehicles along with the collision and connectivity constraints under the predecessor-following architecture for* $N = 100$ *vehicles.*

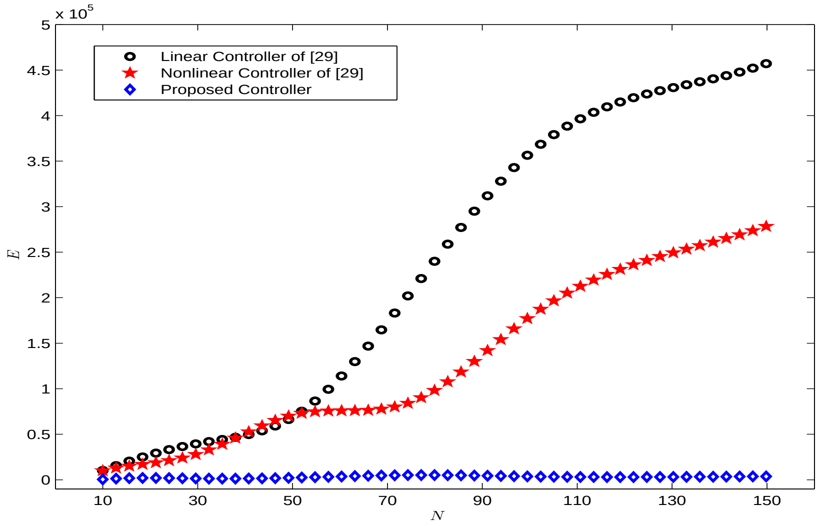

Fig. 3.10: *Comparison of E under the predecessor-following architecture.*

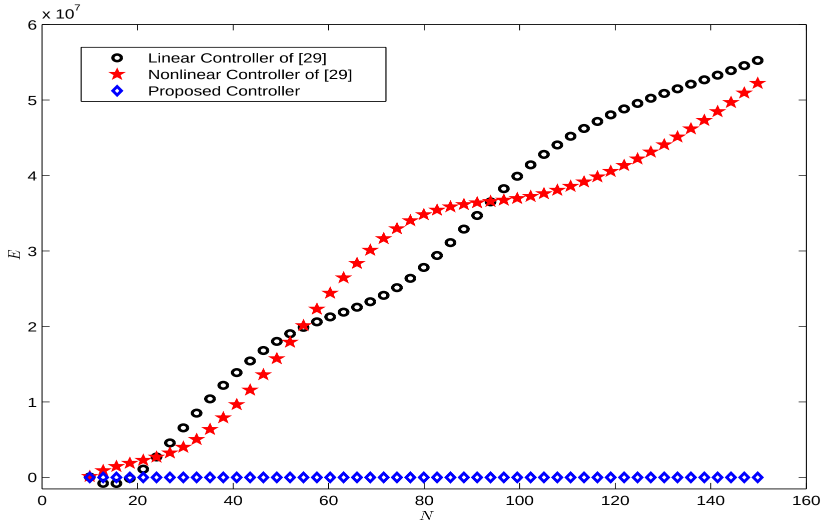

Fig. 3.11: *Comparison of E under the bidirectional architecture.*

Regarding the proposed prescribed performance control scheme, the only parameter changed was the steady state error bound, which was set as $\rho_{inf} = 0.1$m. Finally, the leader node trajectory as well as the desired intervehicular distances were designed in the same way as above. The results of the comparative simulation study are given in Figs. 3.10-3.11 for the predecessor-following and the bidirectional control architecture respectively. Notice that E of the proposed scheme remains practically stable with the increase of N. On the contrary, the figures indicate that the linear and nonlinear methodologies proposed in [29] are highly dependent on the number of vehicles for both control architectures, proving thus the superiority of the proposed method. Finally, while the convergence rate of the presented scheme is solely determined by the term e^{-lt}, the simulation results performed in [29] illustrate that the convergence time may reach more than 80 seconds (see Figs. 2 and 3), resulting in poor control performance.

3.2 2-Dimensional Case

3.2.1 Control Design

The concepts and techniques in the scope of prescribed performance control are innovatively adapted in the 2-dimensional case as well in order to: i) achieve predefined transient and steady state response for the distance and heading errors $e_{d_i}(t)$, $e_{\beta_i}(t)$, $i = 1, \ldots, N$ as defined in (2.10), as well as ii) avoid the violation of the collision and connectivity constraints presented in Section 2.2. Simlarly to the 1-dimensional case, the aforementioned errors will evolve strictly within a predefined region that is bounded by the performance functions. The corresponding mathematical expressions are given by the following inequalities:

$$\left.\begin{array}{l} -\underline{M}_{d_i}\rho_{d_i}(t) < e_{d_i}(t) < \overline{M}_{d_i}\rho_{d_i}(t) \\ -\underline{M}_{\beta_i}\rho_{\beta_i}(t) < e_{\beta_i}(t) < \overline{M}_{\beta_i}\rho_{\beta_i}(t) \end{array}\right\}, \; i = 1, \ldots, N \tag{3.34}$$

for all $t \geq 0$, where

$$\left.\begin{array}{l} \rho_{d_i}(t) = (1 - \frac{\rho_{d,\infty}}{\max\{\underline{M}_{d_i}, \overline{M}_{d_i}\}})e^{-l_d t} + \frac{\rho_{d,\infty}}{\max\{\underline{M}_{d_i}, \overline{M}_{d_i}\}} \\ \rho_{\beta_i}(t) = (1 - \frac{\rho_{\beta,\infty}}{\max\{\underline{M}_{\beta_i}, \overline{M}_{\beta_i}\}})e^{-l_\beta t} + \frac{\rho_{\beta,\infty}}{\max\{\underline{M}_{\beta_i}, \overline{M}_{\beta_i}\}} \end{array}\right\}, \; i = 1, \ldots, N \tag{3.35}$$

are designer-specified, smooth, bounded and decreasing positive functions of time with positive parameters l_j, $\rho_{j,\infty}$, $j \in \{d, \beta\}$ incorporating the desired transient and steady state performance respectively, and $\underline{M}_{j_i}$, $\overline{M}_{j_i}$, $j \in \{d, \beta\}$, $i = 1, \ldots, N$ are positive parameters selected appropriately to satisfy the collision and connectivity constraints, as presented in the sequel. In particular, the decreasing rate of $\rho_{j_i}(t)$, $j \in \{d, \beta\}$, $i = 1, \ldots, N$, which is affected by the constant l_j, $j \in \{d, \beta\}$ introduces a lower bound on the speed of convergence of $e_{j_i}(t)$, $j \in \{d, \beta\}$, $i = 1, \ldots, N$. Furthermore, the constants $\rho_{j,\infty}$, $j \in \{d, \beta\}$ can be set arbitrarily small (i,e, $\rho_{j,\infty} \ll \max\{\underline{M}_{j_i}, \overline{M}_{j_i}\}$, $j \in \{d, \beta\}$, $i = 1, \ldots, N$), thus achieving practical convergence of the distance and heading errors to zero. Additionally, we select:

$$\left.\begin{array}{r} \underline{M}_{d_i} = d_{i,des} - d_{\text{col}} \\ \overline{M}_{d_i} = d_{\text{con}} - d_{i,des} \\ \underline{M}_{\beta_i} = \overline{M}_{\beta_i} = \beta_{\text{con}} \end{array}\right\}, \; i = 1, \ldots, N. \tag{3.36}$$

Notice that the aforementioned parameters d_{con}, β_{con} are related to the constraints imposed by the camera's limited field of view. More specifically, d_{con} should be assigned a value less or equal to the distance from which the marker on the preceding vehicle may be detected by the follower's camera, whereas β_{con} should be less or equal to the half of the camera's angle of view, from which it follows that $\beta_{\text{con}} < \frac{\pi}{2}$ for common cameras. Apparently, since the desired formation is compatible with the collision and connectivity constraints (i.e., $d_{\text{col}} < d_{i,des} < d_{\text{con}}$, $i = 1, \ldots, N$), the aforementioned selection ensures that $\underline{M}_{j_i}, \overline{M}_{j_i} > 0$, $j \in \{d, \beta\}$, $i = 1, \ldots, N$ and consequently under

Assumption A2 that:that:

$$\left.\begin{array}{r}-\underline{M}_{d_i}\rho_{d_i}(0) < e_{d_i}(0) < \overline{M}_{d}\rho_{d_i}(0)\\ -\underline{M}_{\beta_i}\rho_{\beta_i}(0) < e_{\beta_i}(0) < \overline{M}_{\beta}\rho_{\beta_i}(0)\end{array}\right\}, i = 1,\ldots,N. \tag{3.37}$$

Hence, guaranteeing prescribed performance via (3.34) and employing the decreasing property of $\rho_{j_i}(t), j \in \{d,\beta\}, i = 1,\ldots,N$, we conclude:

$$\left.\begin{array}{r}-\underline{M}_{d_i} < e_{d_i}(t) < \overline{M}_{d_i}\\ -\underline{M}_{\beta_i} < e_{\beta_i}(t) < \overline{M}_{\beta_i}\end{array}\right\}, i = 1,\ldots,N$$

and consequently, owing to (3.36):

$$\left.\begin{array}{r}d_{\text{col}} < d_i(t) < d_{\text{con}}\\ -\beta_{\text{col}} < \beta_i(t) < \beta_{\text{con}}\end{array}\right\}, i = 1,\ldots,N$$

and for all $t \geq 0$, which ensures that satisfaction of the collision and connectivity constraints.

In the sequel, we propose a decentralized control protocol without any information on the vehicles' nonlinear model or the external disturbances that guarantees (3.34) for all $t \geq 0$, thus leading to the solution of the 2D formation control problem with prescribed performance under collision and connectivity constraints for the considerd platoon of vehicles.

I. Kinematic Controller

Given the distance and heading errors $e_{j_i}(t), j \in \{d,\beta\}, i = 1,\ldots,N$:

Step I-a. *Select the corresponding performance functions* $\rho_{j_i}(t)$ *and positive parameters* $\underline{M}_{j_i}, \overline{M}_{j_i}, j \in \{d,\beta\}, i = 1,\ldots,N$ *following (3.35) and (3.36) respectively, that incorporate the transient and steady state performance specifications as well as the collision and connectivity constraints.*

Step I-b. *Define the normalized errors as:*

$$\xi_d(e_d,t) = \begin{bmatrix}\xi_{d_1}(e_{d_1},t)\\ \vdots\\ \xi_{d_N}(e_{d_N},t)\end{bmatrix} := \begin{bmatrix}\frac{e_{d_1}}{\rho_{d_1}(t)}\\ \vdots\\ \frac{e_{d_N}}{\rho_{d_N}(t)}\end{bmatrix} \triangleq (\rho_d(t))^{-1}e_d \tag{3.38}$$

$$\xi_\beta(e_\beta,t) = \begin{bmatrix}\xi_{\beta_1}(e_{\beta_1},t)\\ \vdots\\ \xi_{\beta_N}(e_{\beta_N},t)\end{bmatrix} := \begin{bmatrix}\frac{e_{\beta_1}}{\rho_{\beta_1}(t)}\\ \vdots\\ \frac{e_{\beta_N}}{\rho_{\beta_N}(t)}\end{bmatrix} \triangleq (\rho_\beta(t))^{-1}e_\beta \tag{3.39}$$

where $\rho_j(t) = diag([\rho_{j_i}(t)]_{i=1,\ldots,N}), j \in \{d,\beta\}$, *and design the decentralized reference* *angular velocity vector for each wheel:*

$$
\begin{aligned}
\dot{\vartheta}_{R_{des}}(\xi_d, \xi_\beta, t) &= \begin{bmatrix} \dot{\vartheta}_{R_{1,des}}(\xi_{d_1}, \xi_{\beta_1}, t) \\ \vdots \\ \dot{\vartheta}_{R_{N,des}}(\xi_{d_N}, \xi_{\beta_N}, t) \end{bmatrix} = \frac{1}{2}[K_d \varepsilon_d(\xi_d) + K_\beta(\rho_\beta\,(t))^{-1} r_\beta(\xi_\beta)\varepsilon_\beta(\xi_\beta)] \\
\dot{\vartheta}_{L_{des}}(\xi_d, \xi_\beta, t) &= \begin{bmatrix} \dot{\vartheta}_{L_{1,des}}(\xi_{d_1}, \xi_{\beta_1}, t) \\ \vdots \\ \dot{\vartheta}_{L_{N,des}}(\xi_{d_N}, \xi_{\beta_N}, t) \end{bmatrix} = \frac{1}{2}[K_d \varepsilon_d(\xi_d) - K_\beta(\rho_\beta\,(t))^{-1} r_\beta(\xi_\beta)\varepsilon_\beta(\xi_\beta)]
\end{aligned} \tag{3.40}
$$

with $K_j = diag(k_{j_{1,\dots,}} k_{j_N})$, $k_{j_i} > 0, j \in \{d, \beta\}$, $i = 1, \dots, N$, *and*

$$
r_\beta(\xi_\beta) = diag([\frac{\frac{1}{\underline{M}_{\beta_i}} + \frac{1}{\overline{M}_{\beta_i}}}{(1 + \frac{\xi_{\beta_i}}{\underline{M}_{\beta_i}})(1 - \frac{\xi_{\beta_i}}{\overline{M}_{\beta_i}})}]_{i=1,\dots,N}) \tag{3.41}
$$

$$
\varepsilon_d(\xi_d) = \begin{bmatrix} \ln(\frac{1 + \frac{\xi_{d_1}}{\underline{M}_{d_i}}}{1 - \frac{\xi_{d_1}}{\overline{M}_{d_i}}}), \dots, \ln(\frac{1 + \frac{\xi_{d_N}}{\underline{M}_{d_N}}}{1 - \frac{\xi_{d_N}}{\overline{M}_{d_N}}}) \end{bmatrix}^T \tag{3.42}
$$

$$
\varepsilon_\beta(\xi_\beta) = \begin{bmatrix} \ln(\frac{1 + \frac{\xi_{\beta_1}}{\underline{M}_{\beta_i}}}{1 - \frac{\xi_{\beta_1}}{\overline{M}_{\beta_i}}}), \dots, \ln(\frac{1 + \frac{\xi_{\beta_N}}{\underline{M}_{\beta_N}}}{1 - \frac{\xi_{\beta_N}}{\overline{M}_{\beta_N}}}) \end{bmatrix}^T \tag{3.43}
$$

II. Dynamic Controller

Step II-a. *Define the wheel velocity error vector for each vehicle:*

$$
e_{\vartheta_i} = \dot{\vartheta}_i - \dot{\vartheta}_{i,des}(\xi_{d_i}, \xi_{\beta_i}, t),\ i = 1, \dots, N \tag{3.44}
$$

where

$$
\left.\begin{array}{l}
e_{\vartheta_i} = [e_{\vartheta_{R,i}},\ e_{\vartheta_{L,i}}]^T \\
\dot{\vartheta}_i = [\dot{\vartheta}_{R_i},\ \dot{\vartheta}_{L_i}]^T \\
\dot{\vartheta}_{i,des}(\xi_{d_i}, \xi_{\beta_i}, t) = [\dot{\vartheta}_{R_{i,des}}(\xi_{d_i}, \xi_{\beta_i}, t),\ \dot{\vartheta}_{L_{i,des}}(\xi_{d_i}, \xi_{\beta_i}, t)]^T
\end{array}\right\}, \ i = 1, \dots, N
$$

and select the corresponding velocity performance functions

$$
\rho_{\vartheta_i}(t) = \begin{bmatrix} \rho_{\vartheta_{R,i}}(t) & 0 \\ 0 & \rho_{\vartheta_{L,i}}(t) \end{bmatrix},\ i = 1, \dots, N
$$

such that $\rho_{\vartheta_{R,i}}(0) > |e_{\vartheta_{R,i}}(0)|$ *and* $\rho_{\vartheta_{L,i}}(0) > |e_{\vartheta_{L,i}}(0)|$, $i = 1, \dots, N$.

Step II-b. *Define the normalized errors:*

$$
\xi_{\vartheta_i}(e_\vartheta, t) = \begin{bmatrix} \xi_{\vartheta_{R,i}}(e_{\vartheta_{R,i}}, t) \\ \xi_{\vartheta_{L,i}}(e_{\vartheta_{L,i}}, t) \end{bmatrix} \triangleq (\rho_{\vartheta_i}\,(t))^{-1} e_{\vartheta_i},\ i = 1, \dots, N \tag{3.45}
$$

and design the decentralized torque control protocol for each vehicle:

$$\tau_i(\xi_{\vartheta_i},t)=\begin{bmatrix}\tau_{R_i}(\xi_{\vartheta_{R,i}},t)\\ \tau_{L_i}(\xi_{\vartheta_{L,i}},t)\end{bmatrix}=-K_{\vartheta_i}(\rho_{\vartheta_i}(t))^{-1}r_{\vartheta_i}(\xi_{\vartheta_i})\varepsilon_{\vartheta_i}(\xi_{\vartheta_i}),\ i=1,\dots,N \tag{3.46}$$

with

$$K_{\vartheta_i}=\begin{bmatrix}k_{\vartheta_{R,i}} & 0\\ 0 & k_{\vartheta_{L,i}}\end{bmatrix},\ i=1,\dots,N$$

where $k_{\vartheta_{R,i}}>0$, $k_{\vartheta_{L,i}}>0$, $i=1,\dots,N$ *and*

$$r_{\vartheta_i}(\xi_{\vartheta_i})=\begin{bmatrix}\frac{1}{(1-\xi_{\vartheta_{R,i}})(1+\xi_{\vartheta_{R,i}})} & 0\\ 0 & \frac{1}{(1-\xi_{\vartheta_{L,i}})(1+\xi_{\vartheta_{L,i}})}\end{bmatrix} \tag{3.47}$$

$$\varepsilon_{\vartheta_i}(\xi_{\vartheta_i})=\begin{bmatrix}\ln(\frac{1+\xi_{\vartheta_{R,i}}}{1-\xi_{\vartheta_{R,i}}}), & \ln(\frac{1+\xi_{\vartheta_{L,i}}}{1-\xi_{\vartheta_{L,i}}})\end{bmatrix}^T \tag{3.48}$$

for all $i=1,\dots,N$.

Remark 3. *As in the* 1*-dimensional case, equations (3.40) and (3.46) suggest that the proposed control protocol is decentralized in the sense that each vehicle utilizes only local relative to its preceding vehicle information, obtained by its onboard camera, to calculate its own signal, without incorporating any prior information on the vehicle's nonlinear model. Additionally, the transient and steady state performance specifications as well as the collision and connectivity constraints are exclusively introduced by the appropriate selection of* $\rho_{k_i}(t)$, $k\in\{d,\beta,\vartheta\}$ *and* $\underline{M}_{j_i},\overline{M}_{j_i}$, $j\in\{d,\beta\}$, $i=1,\dots,N$.

3.2.2 Stability Analysis

The following theorem summarizes the main results of the 2-dimensional case where it is proven that aforementioned control scheme solves the robust formation problem with prescribed performance under collision and connectivity constraints for the considered platoon of vehicles.

Theorem 3.2. *Consider a platoon of N vehicles with (2.4)-(2.6), following a leader in* 2*-D and aiming at establishing a formation described by the desired inter-vehicular distances* $d_{i,des}$, $i=1,\dots,N$*, while satisfying the collision and connectivity constraints represented by* d_{col} *and* d_{con}, β_{con} *respectively with* $d_{\text{col}}<d_{i,des}<d_{\text{con}}$, $i=1,\dots,N$ *and* $\beta_{\text{con}}<\frac{\pi}{2}$. *Under* ***Assumption A2****, the decentralized control protocol (3.38)-(3.48) guarantees:*

$$\left.\begin{aligned}-\underline{M}_{d_i}\rho_{d_i}(t)<e_{d_i}(t)<\overline{M}_{d_i}\rho_{d_i}(t)\\ -\underline{M}_{\beta_i}\rho_{\beta_i}(t)<e_{\beta_i}(t)<\overline{M}_{\beta_i}\rho_{\beta_i}(t)\end{aligned}\right\},\ i=1,\dots,N$$

for all $t\geq 0$*, as well as the boundedness of all closed loop signals.*

Proof. Differentiating (3.38), (3.39) and (3.45) with respect to time we obtain:

$$\dot{\xi}_d = (\rho_d\,(t))^{-1}(\dot{e}_d - \dot{\rho}_d\,(t)\,\xi_d) \tag{3.49}$$

$$\dot{\xi}_\beta = (\rho_\beta\,(t))^{-1}(\dot{e}_\beta - \dot{\rho}_\beta\,(t)\,\xi_\beta) \tag{3.50}$$

$$\dot{\xi}_{\vartheta_i} = (\rho_{\vartheta_i}\,(t))^{-1}(\dot{e}_{\vartheta_i} - \dot{\rho}_{\vartheta_i}\,(t)\,\xi_{\vartheta_i}), i = 1, \ldots, N. \tag{3.51}$$

Employing (2.6), (2.11), as well as the fact that $\dot{\vartheta}_i = \dot{\vartheta}_{i,des} + \rho_{\vartheta_i}(t)\xi_{\vartheta_i}$, and substituting (3.40) and (3.46) we arrive at:

$$\dot{\xi}_d = h_d(t, \xi_d) = (\rho_d\,(t))^{-1}(-\frac{1}{2}\tilde{C}rK_d\varepsilon_d(\xi_d) + c - \dot{\rho}_d\,(t)\,\xi_d) \tag{3.52}$$

$$\begin{aligned}\dot{\xi}_\beta = h_\beta(t, \xi_d, \xi_\beta) = \frac{1}{2}(\rho_\beta\,(t))^{-1}(-rR^{-1}K_\beta(\rho_\beta\,(t))^{-1}r_\beta(\xi_\beta)\varepsilon_\beta(\xi_\beta) + D^{-1}r\tilde{S}K_d\varepsilon_d(\xi_d) + \\ D^{-1}rs - \dot{\rho}_\beta\,(t)\,\xi_\beta)\end{aligned} \tag{3.53}$$

$$\begin{aligned}\dot{\xi}_{\vartheta_i} = h_{\vartheta_i}(t, \xi_{\vartheta_i}) = -(\rho_{\vartheta_i}\,(t))^{-1}M^{-1}K_{\vartheta_i}(\rho_{\vartheta_i}\,(t))^{-1}r_{\vartheta_i}(\xi_{\vartheta_i})\varepsilon_{\vartheta_i}(\xi_{\vartheta_i}) - (\rho_{\vartheta_i}\,(t))^{-1}(\dot{\rho}_{\vartheta_i}\,(t)\,\xi_{\vartheta_i} - \\ M^{-1}(k_i(\dot{\vartheta}_{i,des} + \rho_{\vartheta_i}(t)\xi_{\vartheta_i}) + n_i(t)) + \ddot{\vartheta}_{i,des})\end{aligned} \tag{3.54}$$

for all $i = 1, \ldots, N$. The closed loop system of $\dot{\xi}_2(t) = [\dot{\xi}_d^T(t), \dot{\xi}_\beta^T(t)]^T$ can be written in compact form as:

$$\dot{\xi}_2(t) = h_3(t, \xi_2) = \begin{bmatrix} h_d(t, \xi_d) \\ h_\beta(t, \xi_d, \xi_\beta) \end{bmatrix}. \tag{3.55}$$

Let us also define the open sets $\Omega_{\xi_2} = \Omega_{\xi_d} \times \Omega_{\xi_\beta} \subset \Re^{2N}$, $\Omega_{\xi_{\theta,i}} \subset \Re^{2N}$ with:

$$\Omega_{\xi_d} = (-\underline{M}_{d_1}, \overline{M}_{d_1}) \times \ldots \times (-\underline{M}_{d_N}, \overline{M}_{d_N})$$

$$\Omega_{\xi_\beta} = \underbrace{(-\underline{M}_{\beta_1}, \overline{M}_{\beta_1}) \times \ldots \times (-\underline{M}_{\beta_N}, \overline{M}_{\beta_N})}_{N\text{-times}}$$

$$\Omega_{\xi_{\theta,i}} = (-1, 1) \times (-1, 1),\ i = 1, \ldots, N.$$

Following the 1-dimensional analysis, in the sequel we proceed in two phases. First, the existence of unique maximal solutions $\xi_2(t)$ of (3.55) over Ω_{ξ_2} and ξ_{ϑ_i} of (3.54) over $\Omega_{\xi_{\theta,i}}$, $i = 1, \ldots, N$ for a time interval $[0, \tau_{\max})$ (i.e., $\xi_2(t) \in \Omega_{\xi_2}$ and $\xi_{\vartheta_i} \in \Omega_{\xi_{\theta,i}}$, $i = 1, \ldots, N$, $\forall t \in [0, \tau_{\max})$) is ensured. Then, we prove that the proposed control scheme guarantees, for all $t \in [0, \tau_{\max})$: a) the boundedness of all closed loop signals as well as that b) $\xi_2(t)$ and ξ_{ϑ_i}, $i = 1, \ldots, N$ remain strictly within compact subsets of Ω_{ξ_2} and $\Omega_{\xi_{\theta,i}}$, $i = 1, \ldots, N$ respectively, which leads by contradiction to $\tau_{\max} = \infty$ and consequently to the completion of the proof.

Phase A. Selecting the parameters $\underline{M}_{j_i}, \overline{M}_{j_i}, j \in \{d, \beta\}, i = 1, \ldots, N$ according to (3.36), we guarantee that the set Ω_{ξ_2} is nonempty and open. Moreover, as shown in (3.37) owing to ***Assumption A2****, $\xi_2(0) \in \Omega_{\xi_2}$. Additionally, h_3 is continuous on t and locally Lipschitz on ξ_2 over the set Ω_{ξ_2}. Therefore, the hypotheses of Theorem 2.3 stated in Appendix B′ hold and the existence of a maximal solution $\xi_2(t)$ of (3.55) for a time interval $[0, \tau_{\max})$ such that $\xi_2(t) \in \Omega_{\xi_2}$, $\forall t \in [0, \tau_{\max})$ is guaranteed. In the same vein, by selecting $\rho_{\vartheta_i}(t)$ such that $\rho_{\vartheta_{R,i}}(0) > |e_{\vartheta_{R,i}}(0)|$ and $\rho_{\vartheta_{L,i}}(0) > |e_{\vartheta_{L,i}}(0)|$, $i = 1, \ldots, N$, we guarantee that*

$\xi_{\vartheta_i}(0) \in \Omega_{\xi_{\theta,i}}$, $i = 1, \dots, N$ as well. Since the functions h_{ϑ_i} are locally Lipschitz on ξ_{ϑ_i}, $i = 1, \dots, N$, we deduce the existence of a maximal solution $\xi_{\vartheta_i}(t)$ of (3.54) for each $i = 1, \dots, N$ and $\forall t \in [0, \tau_{\max})$ such that $\xi_{\vartheta_i} \in \Omega_{\xi_{\theta,i}}$, $i = 1, \dots, N$.

Phase B. We have proven in Phase A that $\xi_2(t) \in \Omega_{\xi_2}$ and $\xi_{\vartheta_i} \in \Omega_{\xi_{\theta,i}}$, $i = 1, \dots, N$, $\forall t \in [0, \tau_{\max})$ and more specifically that:

$$\left.\begin{aligned} \xi_{d_i} &= \frac{e_{d_i}(t)}{\rho_{d_i}(t)} \in (-\underline{M}_{d_i},\ \overline{M}_{d_i}) \\ \xi_{\beta_i} &= \frac{e_{\beta_i}(t)}{\rho_{\beta_i}(t)} \in (-\underline{M}_{\beta_i},\ \overline{M}_{\beta_i}) \\ \xi_{\vartheta_{R,i}} &= \frac{e_{\vartheta_{R,i}}(t)}{\rho_{\vartheta_{R,i}}(t)} \in (-1,\ 1) \\ \xi_{\vartheta_{L,i}} &= \frac{e_{\vartheta_{L,i}}(t)}{\rho_{\vartheta_{L,i}}(t)} \in (-1,\ 1) \end{aligned}\right\} i = 1, \dots, N \tag{3.56}$$

for all $t \in [0, \tau_{\max})$, from which we obtain that $e_{d_i}(t)$, $e_{\beta_i}(t)$, $e_{\vartheta_{R,i}}(t)$ and $e_{\vartheta_{L,i}}(t)$ are absolutely bounded by $\max\{\underline{M}_{d_i}, \overline{M}_{d_i}\}\rho_{d_i}(t)$, $\max\{\underline{M}_{\beta_i}, \overline{M}_{\beta_i}\}\rho_{\beta_i}(t)$, $\rho_{\vartheta_{R,i}}(t)$ and $\rho_{\vartheta_{L,i}}(t)$ respectively for $i = 1, \dots, N$. Let us also define:

$$r_d(\xi_d) = diag([\frac{\frac{1}{\underline{M}_{d_i}} + \frac{1}{\overline{M}_{d_i}}}{(1 + \frac{\xi_{d_i}}{\underline{M}_{d_i}})(1 - \frac{\xi_{d_i}}{\overline{M}_{d_i}})}]_{i=1,\dots,N}). \tag{3.57}$$

Now, assume there exists a set $I \subseteq \{1, \dots, N\}$ such that $\lim_{t \to \tau_{\max}} \xi_{d_k} = \overline{M}_{d_k}$ (or $-\underline{M}_{d_k}$). Hence, invoking (3.42) and (3.57), we conclude that $\lim_{t \to \tau_{\max}} \varepsilon_{d_d}(\xi_{d_k}(t)) = +\infty$ (or $-\infty$) and $\lim_{t \to \tau_{\max}} r_{d_k}(\xi_{d_k}(t)) = +\infty$, $\forall k \in I$. Moreover, we also deduce from (3.40) that $\lim_{t \to \tau_{\max}} \dot{\vartheta}_{R_k}(\xi_{d_k}, \xi_{\beta_k}, t)$ and $\lim_{t \to \tau_{\max}} \dot{\vartheta}_{L_k}(\xi_{d_L}, \xi_{\beta_L}, t)$ remain bounded for all $k \in \bar{I}$, where $\bar{I}$ is the complementary set ot I. To proceed, let us define $\bar{k} = \min\{I\}$ and notice that $\varepsilon_{d_{\bar{d}}}(\xi_{d_{\bar{k}}})$, as derived from (3.42), is well defined for all $t \in [0, \tau_{\max})$, owing to (3.56). Therefore, consider the positive definite and radially ubounded function $V_{d_{\bar{k}}} = \frac{1}{2}\,\varepsilon^2_{d_{\bar{d}}}$ for which it is clear that $\lim_{t \to \tau_{\max}} V_{d_{\bar{k}}}(t) = +\infty$. However, differentiating $V_{d_{\bar{k}}}$ with respect to time and substituting (2.10), we obtain:

$$\dot{V}_{d_{\bar{k}}} = \varepsilon_{d_{\bar{d}}} r_{d_{\bar{k}}}(\xi_{d_{\bar{k}}})(\rho_{d_{\bar{k}}}(t))^{-1}(-\frac{r_{\bar{k}}}{2}(\dot{\vartheta}_{R_{\bar{k}}} + \dot{\vartheta}_{L_{\bar{k}}}) \cos\beta_{\bar{k}} + \frac{r_{\bar{k}}}{2}(\dot{\vartheta}_{R_{\bar{k}-1}} + \dot{\vartheta}_{L_{\bar{k}-1}}) \cos(\gamma_{\bar{k}} + \beta_{\bar{k}}) - \dot{\rho}_{d_{\bar{k}}}(t)\,\xi_{d_{\bar{k}}})$$

from which, owing to the fact that $\frac{r_{\bar{k}}}{2}(\dot{\vartheta}_{R_{\bar{k}-1}} + \dot{\vartheta}_{L_{\bar{k}-1}}) \cos(\gamma_{\bar{k}} + \beta_{\bar{k}}) - \dot{\rho}_{d_{\bar{k}}}(t)\,\xi_{d_{\bar{k}}})$ is bounded, since $\bar{k} - 1 \in \bar{I}$, and $\cos\beta_{\bar{k}} > \cos\beta_{\text{con}} > 0$, we conclude that $\lim_{t \to \tau_{\max}} \dot{V}_{d_{\bar{k}}}(t) = -\infty$, which clearly contradicts to our supposition that $\lim_{t \to \tau_{\max}} V_{d_{\bar{k}}}(t) = +\infty$. Thus, we conclude that $\bar{k}$ does not exist and hence that I is an empty set. Therefore, there exist $\underline{\xi}_{d_i}$ and $\overline{\xi}_{d_i}$ such that:

$$-\underline{M}_{d_i} < \underline{\xi}_{d_i} \leq \xi_{d_i}(t) \leq \overline{\xi}_{d_i} < \overline{M}_{d_i},\ \forall t \in [0, \tau_{\max}) \tag{3.58}$$

for all $i = 1, \dots, N$ and $\forall t \in [0, \tau_{\max})$.

Notice also from (3.56) that $\varepsilon_\beta(\xi_\beta)$, as derived from (3.43), is well defined for all $t \in [0, \tau_{\max})$. Therefore, consider the positive definite and radially unbouded function $V_\beta = \frac{1}{2}\varepsilon_\beta^T K_\beta^{-1} \varepsilon_\beta$. Differentiating V_β with respect to time and substituting (3.53), we obtain:

$$\dot{V}_\beta = -\frac{1}{2}\left\|\varepsilon_\beta^T(\xi_\beta) r_\beta(\xi_\beta)(\rho_\beta(t))^{-1}\right\|^2 + \frac{1}{2}\varepsilon_\beta^T(\xi_\beta) r_\beta(\xi_\beta)(\rho_\beta(t))^{-1} K_\beta^{-1}[D^{-1} r(\tilde{S} K_d \varepsilon_d(\xi_d) + s) - \dot{\rho}_\beta(t)\,\xi_d].$$

Hence, exploiting the boundedness of D^{-1}, $\tilde{S}$, s *and* $\varepsilon_d(\xi_d)$, *we get:*

$$\dot{V}_\beta \le -\frac{1}{2}\left\|\varepsilon_\beta^T(\xi_\beta)r_\beta(\xi_\beta)(\rho_\beta(t))^{-1}\right\|^2 + \frac{1}{2}\left\|\varepsilon_\beta^T(\xi_\beta)r_\beta(\xi_\beta)(\rho_\beta(t))^{-1}\right\|\bar{F}_\beta \tag{3.59}$$

where $\bar{F}_\beta$ *is a positive constant independent of* $\tau_{\max}$, *satisfying:*

$$\left\|K_\beta^{-1}[D^{-1}r(\tilde{S}K_d\varepsilon_d(\xi_d)+s)-\dot{\rho}_\beta(t)\,\xi_d]\right\| \le \bar{F}_\beta \tag{3.60}$$

for all $\xi_2(t)\in\Omega_{\xi_2}$. *Therefore, we conclude that* $\dot{V}_\beta$ *is negative when* $\left\|\varepsilon_\beta^T(\xi_\beta)r_\beta(\xi_\beta)(\rho_\beta(t))^{-1}\right\| > \bar{F}_\beta$, *from which, owing to the positive definiteness and diagonality of* $r_\beta(\xi_\beta)(\rho_\beta(t))^{-1}$ *as well as employing (3.35) and (3.41), it can be easily verified that:*

$$\|\varepsilon_\beta(t)\| \le \bar{\varepsilon}_\beta := \max\left\{\|\varepsilon_\beta(0)\|, \bar{F}_\beta \max\left\{\frac{\underline{M}_{\beta_i}\overline{M}_{\beta_i}}{\underline{M}_{\beta_i}+\overline{M}_{\beta_i}}\right\}\right\}$$

for all $t\in[0,\tau_{\max})$. *Furthermore, invoking the inverse algorithm in (3.43), we obtain:*

$$-\underline{M}_{\beta_i} < \frac{e^{-\bar{\varepsilon}_\beta}-1}{e^{-\bar{\varepsilon}_\beta}+1}\underline{M}_{\beta_i} = \underline{\xi}_{\beta_i} \le \xi_{\beta_i}(t) \le \bar{\xi}_{\beta_i} = \frac{e^{\bar{\varepsilon}_\beta}-1}{e^{\bar{\varepsilon}_\beta}+1}\overline{M}_{\beta_i} < \overline{M}_{\beta_i} \tag{3.61}$$

for all $t\in[0,\tau_{\max})$ *and* $i=1,\dots,N$. *From (3.58) and (3.61) it can be easily deduced that the desired angular velocities as designed in (3.40) are bounded for all* $t\in[0,\tau_{\max})$. *Moreover, invoking* $\dot{\vartheta}_i=\dot{\vartheta}_{i,des}+\rho_{\vartheta_i}(t)\xi_{\vartheta_i}$, $i=1,\dots,N$ *we also conclude the boundedness of the velocities* $\dot{\vartheta}_i=[\dot{\vartheta}_{R_i},\dot{\vartheta}_{L_i}]^T$, $i=1,\dots,N$ *for all* $t\in[0,\tau_{\max})$. *Finally, notice by (3.40) that the time derivative of* $\dot{\vartheta}_{i,des}$ *is a function of* $\xi_{d_i},\dot{\xi}_{d_i},\xi_{\beta_i},\dot{\xi}_{\beta_i}$ *which are proven to be bounded for all* $t\in[0,\tau_{\max})$ *and* $i=1,\dots,N$ *(see (3.52), (3.53), (3.58) and (3.61)). Hence, we conclude the boundedness of* $\ddot{\vartheta}_{i,des}$ *for all* $t\in[0,\tau_{\max})$, $i=1,\dots,N$ *as well.*

Applying the aforentioned line of proof, we consider positive definite and radially undounded functions $V_{\vartheta_i}=\frac{1}{2}\varepsilon_{\vartheta_i}^T\varepsilon_{\vartheta_i}$, $i=1,\dots,N$. *Differentiating* V_{ϑ_i} *with respect to time and employing (3.54), we obtain:*

$$\begin{aligned}\dot{V}_{\vartheta_i} = {}& -\varepsilon_{\vartheta_i}^T r_{\vartheta_i}(\xi_{\vartheta_i})(\rho_{\vartheta_i}(t))^{-1}M^{-1}K_{\vartheta_i}(\rho_{\vartheta_i}(t))^{-1}r_{\vartheta_i}(\xi_{\vartheta_i})\varepsilon_{\vartheta_i} + \varepsilon_{\vartheta_i}^T r_{\vartheta_i}(\xi_{\vartheta_i})(\rho_{\vartheta_i}(t))^{-1}(\dot{\rho}_{\vartheta_i}(t)\,\xi_{\vartheta_i} - \\ & M^{-1}(k_i(\dot{\vartheta}_{i,des}+\rho_{\vartheta_i}(t)\xi_{\vartheta_i})+n_i(t))+\ddot{\vartheta}_{i,des})\end{aligned}$$

for all $i=1,\dots,N$. *Hence, exploiting the positive definiteness of* $M^{-1}K_{\vartheta_i}$ *as well as the boundedness of* $\rho_{\vartheta_i}(t)$, $\dot{\rho}_{\vartheta_i}(t)$, $\dot{\vartheta}_{i,des}+\rho_{\vartheta_i}(t)\xi_{\vartheta_i}$, $n_i(t)$ *and* $\ddot{\vartheta}_{i,des}$, $i=1,\dots,N$ *we conclude that:*

$$\dot{V}_{\vartheta_i} \le -\lambda_{\min}(M^{-1}K_{\vartheta_i})\left\|\varepsilon_{\vartheta_i}^T r_{\vartheta_i}(\xi_{\vartheta_i})(\rho_{\vartheta_i}(t))^{-1}\right\|^2 + \left\|\varepsilon_{\vartheta_i}^T r_{\vartheta_i}(\xi_{\vartheta_i})(\rho_{\vartheta_i}(t))^{-1}\right\|\bar{F}_\vartheta$$

where $\bar{F}_\vartheta$ *is a positive constant independent of* $\tau_{\max}$, *satisfying*

$$\left\|\dot{\rho}_{\vartheta_i}(t)\,\xi_{\vartheta_i} - M^{-1}(k_i(\dot{\vartheta}_{i,des}+\rho_{\vartheta_i}(t)\xi_{\vartheta_i})+n_i(t))+\ddot{\vartheta}_{i,des}\right\| \le \bar{F}_\vartheta \tag{3.62}$$

for all $i=1,\dots,N$. *Therefore, we conclude that* $\dot{V}_{\vartheta_i}$ *is negative when* $\left\|\varepsilon_{\vartheta_i}^T r_{\vartheta_i}(\xi_{\vartheta_i})(\rho_{\vartheta_i}(t))^{-1}\right\| >$

$\frac{\bar{F}_{\vartheta}}{\lambda_{\min}(M^{-1}K_{\vartheta_i})}$, $i = 1, \ldots, N$ from which we can arrive at:

$$\|\varepsilon_{\vartheta_i}(t)\| \leq \bar{\varepsilon}_{\vartheta_i} := \max\left\{\|\varepsilon_{\vartheta_i}(0)\|, \frac{\bar{F}_{\vartheta}}{\lambda_{\min}(M^{-1}K_{\vartheta_i})}\right\}, i = 1, \ldots, N$$

for all $t \in [0, \tau_{\max})$. Hence, invoking the inverse logarithm in (3.48), we obtain:

$$\begin{aligned} -1 < \frac{e^{-\bar{\varepsilon}_{\vartheta_i}} - 1}{e^{-\bar{\varepsilon}_{\vartheta_i}} + 1} = \underline{\xi}_{\vartheta_i} \leq \xi_{\vartheta_{R,i}}(t) \leq \bar{\xi}_{\vartheta_i} = \frac{e^{\bar{\varepsilon}_{\vartheta_i}} - 1}{e^{\bar{\varepsilon}_{\vartheta_i}} + 1} < 1 \\ -1 < \frac{e^{-\bar{\varepsilon}_{\vartheta_i}} - 1}{e^{-\bar{\varepsilon}_{\vartheta_i}} + 1} = \underline{\xi}_{\vartheta_i} \leq \xi_{\vartheta_{L,i}}(t) \leq \bar{\xi}_{\vartheta_i} = \frac{e^{\bar{\varepsilon}_{\vartheta_i}} - 1}{e^{\bar{\varepsilon}_{\vartheta_i}} + 1} < 1 \end{aligned} \tag{3.63}$$

for all $t \in [0, \tau_{\max})$ and $i = 1, \ldots, N$, which also leads to the boundedness of the distributed torque control protocol (3.46).

Up to this point, what remains to be shown is that $\tau_{\max}$ can be extended to ∞. In this direction, notice by (3.58), (3.61) and (3.63) that $\xi_2(t) \in \Omega'_{\xi_2} = \Omega'_{\xi_d} \times \Omega'_{\xi_\beta}$ and $\xi_{\vartheta_i}(t) \in \Omega'_{\xi_{\theta,i}}$, $i = 1, \ldots, N$, $\forall t \in [0, \tau_{\max})$, where

$$\begin{aligned} \Omega'_{\xi_d} &= (\underline{\xi}_{d_1}, \bar{\xi}_{d_1}) \times \ldots \times (\underline{\xi}_{d_N}, \bar{\xi}_{d_N}) \\ \Omega'_{\xi_\beta} &= (\underline{\xi}_{\beta_1}, \bar{\xi}_{\beta_1}) \times \ldots \times (\underline{\xi}_{\beta_N}, \bar{\xi}_{\beta_N}) \\ \Omega'_{\xi_{\theta,i}} &= (\underline{\xi}_{\vartheta_i}, \bar{\xi}_{\vartheta_i}) \times (\underline{\xi}_{\vartheta_i}, \bar{\xi}_{\vartheta_i}), \; i = 1, \ldots, N \end{aligned}$$

are nonempty and compact subsets of Ω_{ξ_d}, Ω_{ξ_β} and $\Omega_{\xi_{\theta,i}}$, $i = 1, \ldots, N$ respectively. Hence, assuming that $\tau_{\max} < \infty$ and since $\Omega'_{\xi_2} \subset \Omega_{\xi_2}$ and $\Omega'_{\xi_{\theta,i}} \subset \Omega_{\xi_{\theta,i}}$, $i = 1, \ldots, N$, Proposition 2.1 in Appendix B′ dictates the existence of a time instant $t' \in [0, \tau_{\max})$ such that $\xi_2(t') \notin \Omega'_{\xi_2}$ and $\xi_{\vartheta_i}(t') \notin \Omega'_{\xi_{\theta,i}}$, $i = 1, \ldots, N$ which is a clear contradiction. Therefore, $\tau_{\max} = \infty$. Thus, all closed loop signals remain bounded and moreover $\xi_2(t) \in \Omega'_{\xi_2} \subset \Omega_{\xi_2}$ and $\xi_{\vartheta_i}(t) \in \Omega'_{\xi_{\theta,i}} \subset \Omega_{\xi_{\theta,i}}$, $i = 1, \ldots, N$ for all $t \geq 0$. Finally, multiplying (3.58) and (3.61) by $\rho_{d_i}(t)$ and $\rho_{\beta_i}(t)$ respectively, we conclude:

$$\left.\begin{aligned} -\underline{M}_{d_i}\rho_{d_i}(t) < e_{d_i}(t) < \overline{M}_{d_i}\rho_{d_i}(t) \\ -\underline{M}_{\beta_i}\rho_{\beta_i}(t) < e_{\beta_i}(t) < \overline{M}_{\beta_i}\rho_{\beta_i}(t) \end{aligned}\right\}, \; t \geq 0 \tag{3.64}$$

for all $i = 1, \ldots, N$ and consequently the solution of the formation control problem with prescribed performance under collision and connectivity constraints for the considered platoon of vehicles.

Remark 4. *Identical conclusions can be drawn in the 2-dimensional case as well. In particular, notice that there is no need to render the transformed errors $e_d(t)$, $e_\beta(t)$ and $e_{\vartheta_i}(t)$, $i = 1, \ldots, N$ arbitrarily small, since (3.58), (3.61) and (3.63) hold no matter how large the finite bounds $\underline{\xi}_{d_i}$, $\bar{\xi}_{d_i}$, $\underline{\xi}_{\beta_i}$, $\bar{\xi}_{\beta_i}$, $\underline{\xi}_{\vartheta_i}$, $\bar{\xi}_{\vartheta_i}$ are. The actual performance given in (3.64) is solely determined by the designer-specified functions $\rho_{d_i}(t)$, $\rho_{\beta_i}(t)$ and parameters $\underline{M}_{d_i}$, $\overline{M}_{d_i}$, $\underline{M}_{\beta_i}$, $\overline{M}_{\beta_i}$, that are related to the collision and connectivity constraints. Regarding the control gain K_d, K_β, K_{ϑ_i} selection, fine tuning might be needed in real-time scenarios, to constrain the linear and angular velocities within the range of velocities the motors are*

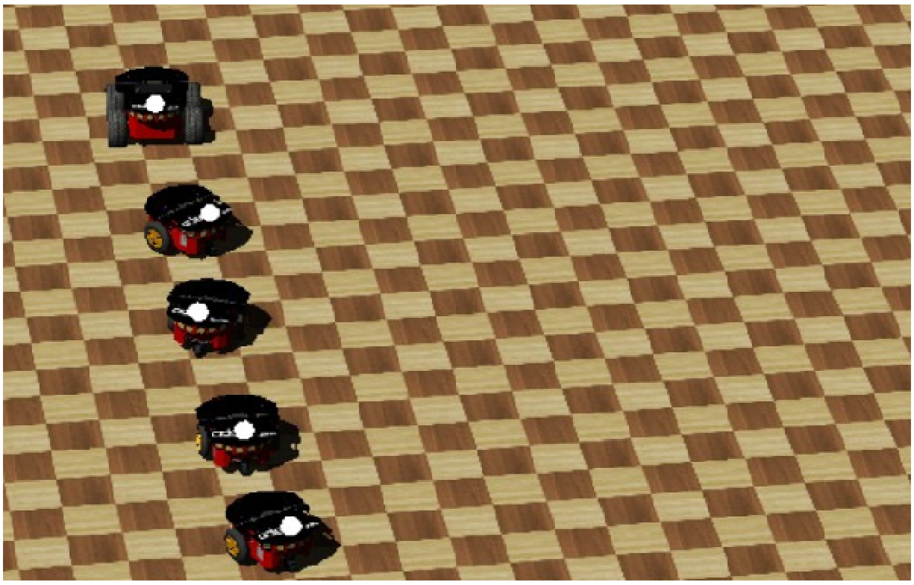

Fig. 3.12: *Intial pose of the platoon vehicles in the WEBOTS^{TM} simulation.*

able to achieve. Similarly, the control input constraints impose an upper bound on the required speed of convergence of $\rho_{j_i}(t)$, $i = 1, \ldots, N$, as obtained by the exponentials $e^{-l_j t}, j \in \{d, \beta\}$.

Remark 5. *Notice that from eq. (2.2), which holds for both 1-D and 2-D cases (note however the change of notation to e_d instead of e_p in the 2-D case), the following inequality can be derived:*

$$\|e_{p_0}\| \le \frac{\|e_p\|}{\sigma_{\min}(S)},\ \forall t \ge 0 \tag{3.65}$$

where $e_{p_0} = [e_{p_{0,1}}, \cdots, e_{p_{0,N}}]^T$ is the error with respect to leading vehicle and $\sigma_{\min}(\cdot)$ denotes the minimum singular value. Moreover, it is straightforward from the aforementioned analysis that the steady state errors satisfy the relation $\left|e^{ss}_{p_i}\right| \le \rho_\infty$, ,$i = 1, \ldots, N$ and hence$\left\|e^{ss}_p\right\| \le \rho_\infty\sqrt{N}$, where the superscript ss denotes the steady state. Eq. (3.65) becomes therefore

$$\left\|e^{ss}_{p_0}\right\| \le \frac{\rho_\infty\sqrt{N}}{\sigma_{\min}(S)}$$

which suggests that the value of ρ_∞ can be selected so that predefined convergence of $e^{ss}_{p_0}$ is attained. For instance, seting $\rho_\infty = \rho_{\infty_0}\sigma_{\min}(S)$ will achieve the convergence of $\left\|e^{ss}_{p_0}\right\|$ to $\rho_{\infty_0}\sqrt{N}$ and consequently:

$$\left|e^{ss}_{p_{0,i}}\right| \le \rho_{\infty_0},\ i = 1, \ldots, N$$

where ρ_{∞_0} can be set arbitrarily small.

3.2.3 Simulations

To demonstrate the efficiency of the proposed decentralized control protocol, a realistic simulation was carried out in the WEBOTS^{TM} platform [70], considering a platoon comprising of a Pioneer3AT/leader and 7 Pioneer3DX following vehicles that utilize the kinematic controller (3.38)-(3.43) in velocity-control mode. The inter-vehicular distance and the bearing angle are obtained by a camera with range $D = 2m$ and angle of view $AoV = 90^o$, that is mounted on each Pioneer3DX vehicle and detects a white spherical marker attached on its predecessor. The initial pose of all vehicles is illustrated in Fig. 3.12. The leader vehicle performs a smooth maneuver depicted in Fig. 3.13, along with the trajectories of the folloing vehicles. The desired distance between successive vehicles is set equally at $d_{i,des} = d = 0.75m$, $i = 1, \ldots, N$, whereas the collision and connectivity constraints are given by $d_{\text{col}} = 0.05d = 0.0375m$ and $d_{\text{con}} = D = 2m$. Regarding the heading error, we select $\beta_{\text{con}} = \frac{AoV}{2} = 45^o$. In addition, we require steady state error of no more than $0.0625m$ and minimum speed of convergence as obtained by the exponential $e^{-0.5t}$ for the distance error. Thus, invoking (3.36), we select the parameters $\underline{M}_{d_i} = 0.7125m$, $\overline{M}_{d_i} = 1.25m$ and the functions $\rho_{d_i}(t) = (1 - \frac{0.0625}{1.25})e^{-0.5t} + \frac{0.0625}{1.25}$, $i = 1, \ldots, N$. In the same vein, we require maximum steady state error of 1.15^o and minimum speed of convergence as obtained by the exponential $e^{-0.5t}$ for the heading error. Therefore, $\underline{M}_{\beta_i} = \overline{M}_{\beta_i} = \beta_{\text{con}} = 45^o$ and $\rho_{\beta_i}(t) = (1 - \frac{1.15}{45})e^{-0.5t} + \frac{1.15}{45}$, $i = 1, \ldots, N$. Finally, we chose $K_d = diag[0.005, \ldots, 0.005]$ and $K_\beta = diag[0.001, \ldots, 0.001]$ to produce reasonable linear and angular velocities within the feasible sets of the mobile robots.

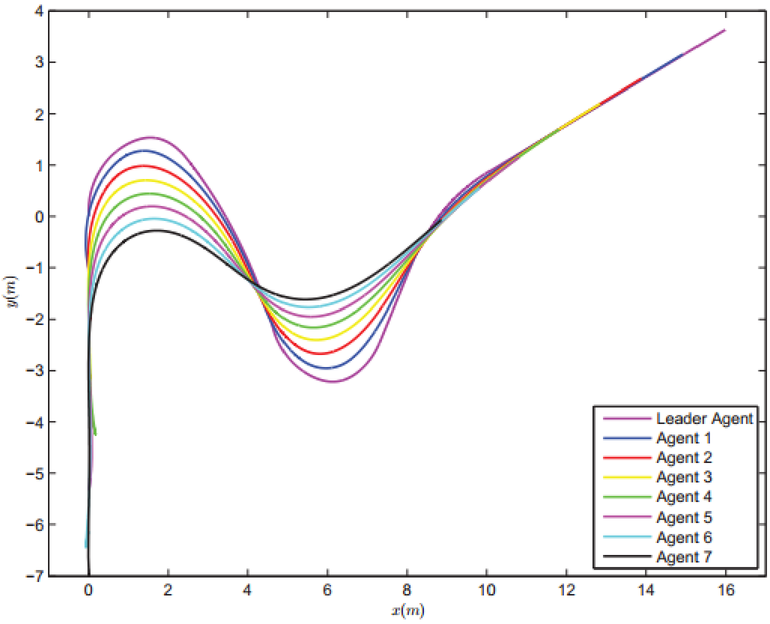

Fig. 3.13: *The trajectories on a planar surface of the vehicles composing the platoon.*

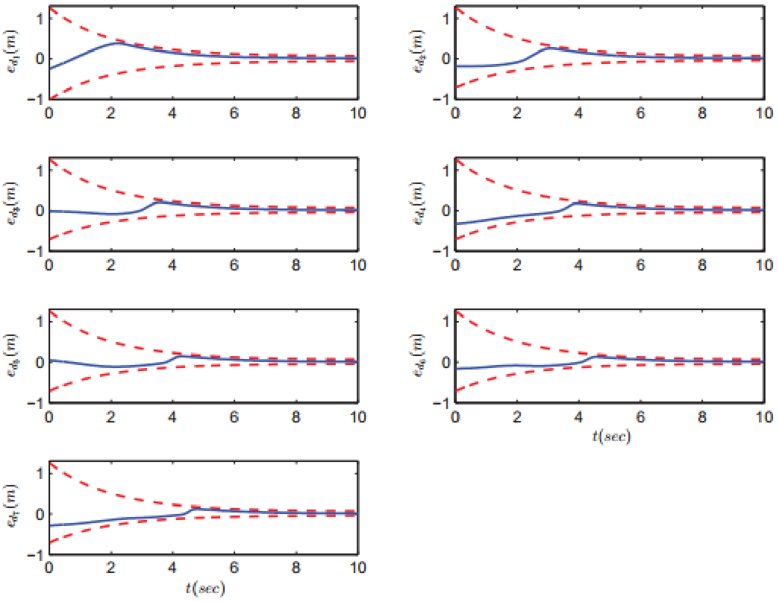

Fig. 3.14: *The evolution of the distance errors* $e_{d_i}(t), i = 1, \ldots, 7$ *(blue lines), along with the imposed performance bounds (red lines).*

The simulation results are illustrated in Figs. 3.14-3.17. More specifically, the evolution of the distance and heading errors $e_{d_i}(t)$, $e_{\beta_i}(t)$, $i = 1, \ldots, 7$ is depicted in Figs. 3.14 and 3.15 respectively, along with the corresponding perfrormance bounds. The inter-vehicular distance along with the collision and connectivity constraints are pictured in Fig. 3.16. Moreover, Fig. 3.17 shows the orientation of each vehicle. As it was predicted by the theoretical analysis, the decentralized $2 - D$ contol problem of vehicular platoons under limited visual feedback is solved with guaranteed transient and steady state response as well as collision avoidance and connectivity maintenance. Finally, Figs. 3.18 and 3.19 depict snapshots of the platoon at several time instants.

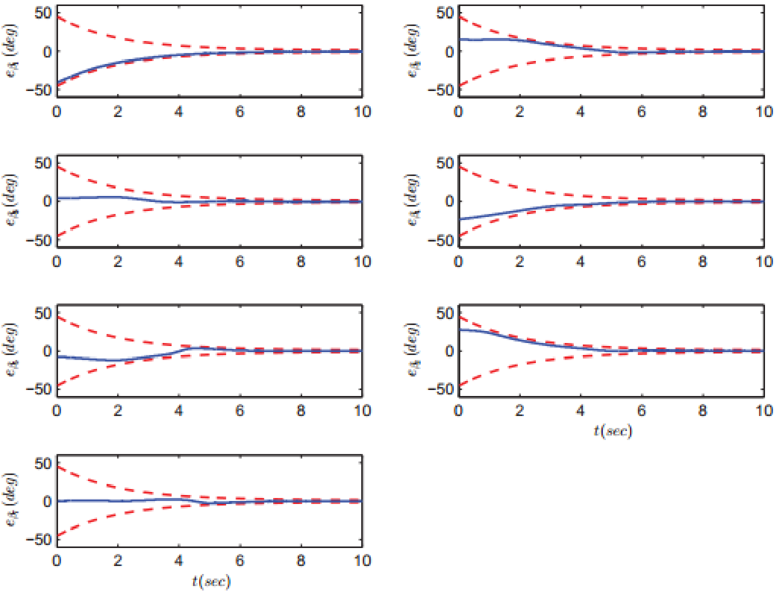

Fig. 3.15: *The evolution of the heading errors* $e_{\beta_i}(t)$*,* $i = 1, \dots, 7$ *(blue lines), along with the imposed performance boundes (red lines).*

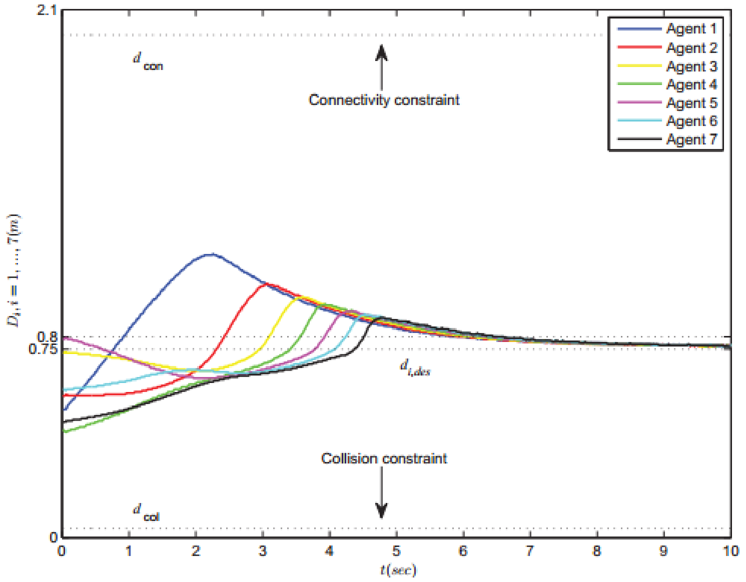

Fig. 3.16: *The distance between successive vehicles along with the collision and connectivity constraints.*

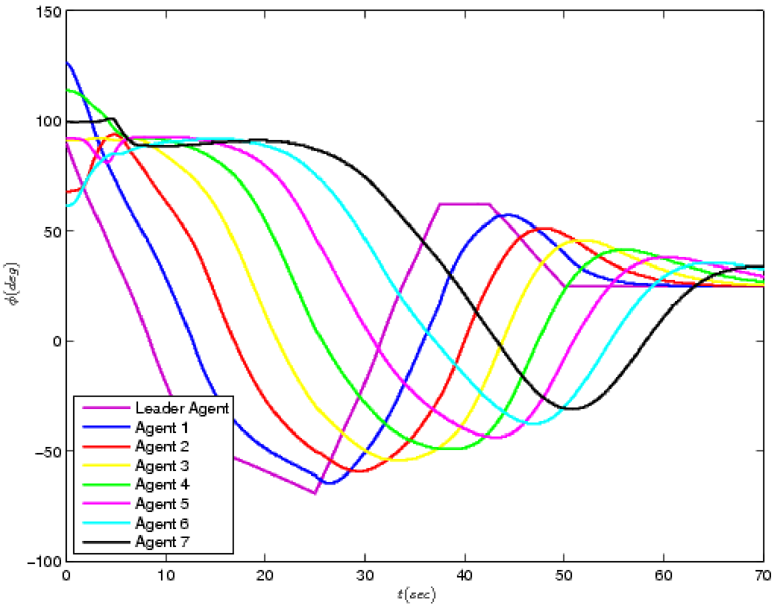

Fig. 3.17: *The orientation angle of each vehicle.*

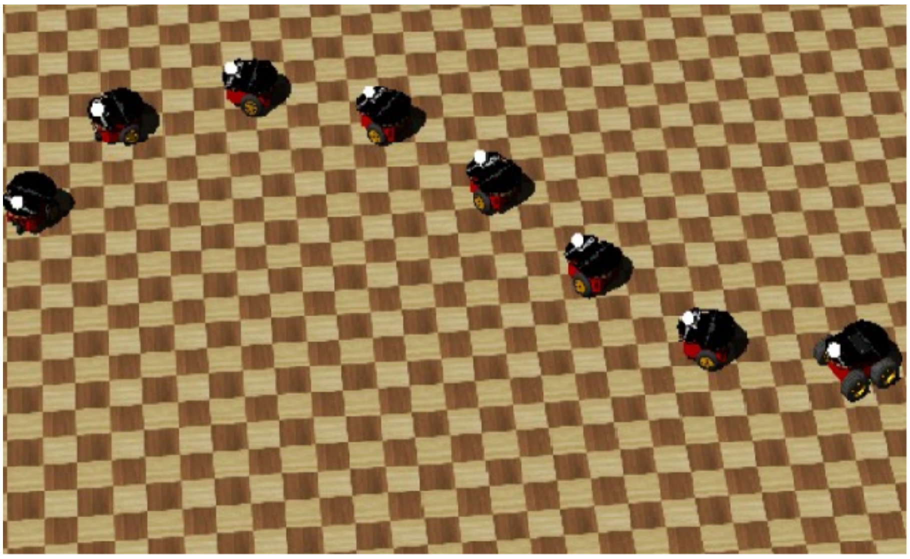

Fig. 3.18: *Snapshot of the 2-D vehicle platoon simulation in WEBOTS^{TM}.*

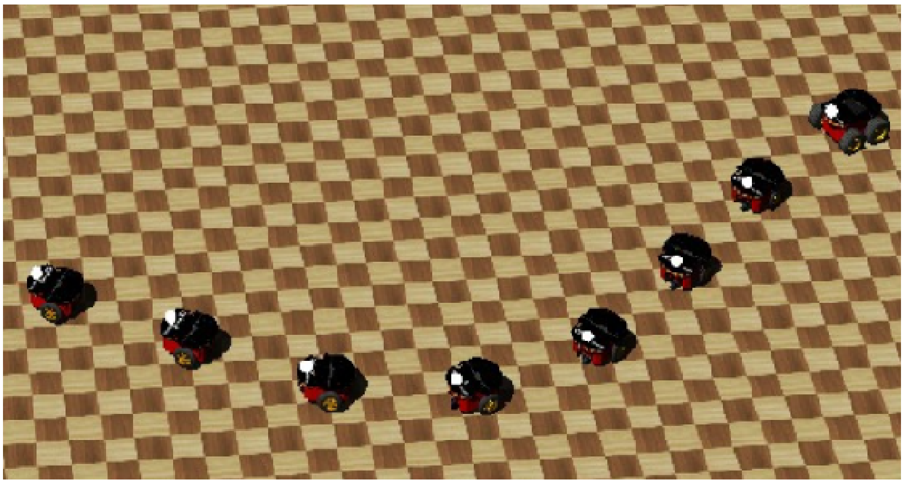

Fig. 3.19: *Snapshot of the 2-D vehicle platoon simulation in WEBOTS*^{TM}.

Chapter 4

Experimental Evaluation

To illustrate further the performance and the robustness of the proposed control scheme, an experimental procedure was carried out for the case of the predecessor-following architecture, utilizing the kinematic part of the control protocol as designed in section 3.1. The experiment took place along a 10m long hallway and lasted approximately 18 seconds.

4.1 System Components

For the composition of the vehicle platoon, five mobile robots were employed. A PIonner 2AT was utilized as leader vehicle and two KUKA Youbots along with two Pionner 2DX mobile robots consisted the following vehicles (see Figs. 4.1-4.3) forming a platoon of 2.5m long. By choosing the desired distances between consecutive vehicles at $\Delta_{i-1,i} = \Delta^* = 0.2\text{m}$, $i = 1, \ldots, 4$, the platoon was able to perform a longitudinal course of approximately 5.5m. bla bla . For the feedback of the intervehicular distance, four infrared proximity sensors ranging from 5cm to 80cm were used. The analog voltage output of the sensors was transferred to the vehicle computers via an Arduino microcontroller. The system software was implemented in Python programming language and the operating system was linux.

Fig. 4.1: *A Pioneer 2AT mobile robot.*

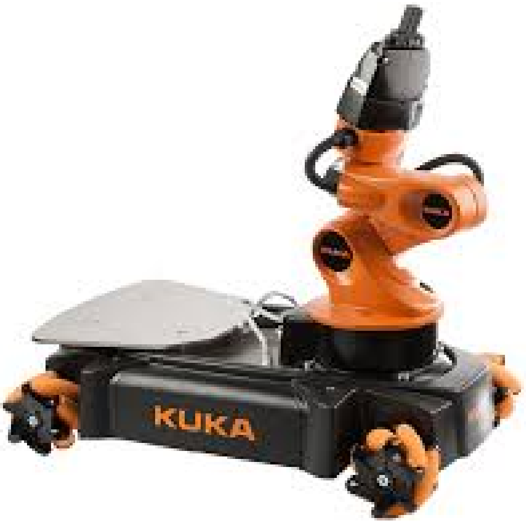

Fig. 4.2: *A KUKA Youbot.*

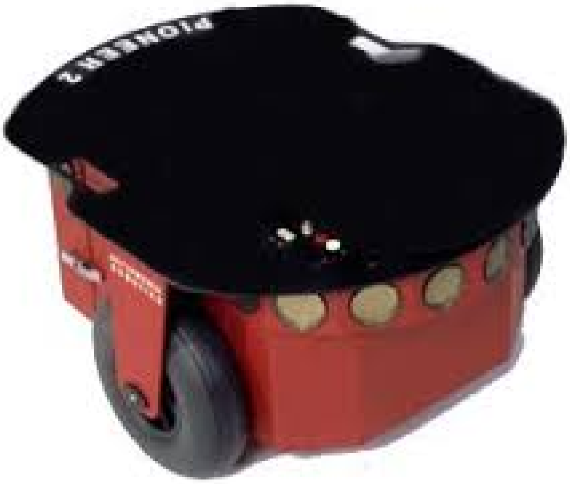

Fig. 4.3: *A Pioneer 2DX mobile robot.*

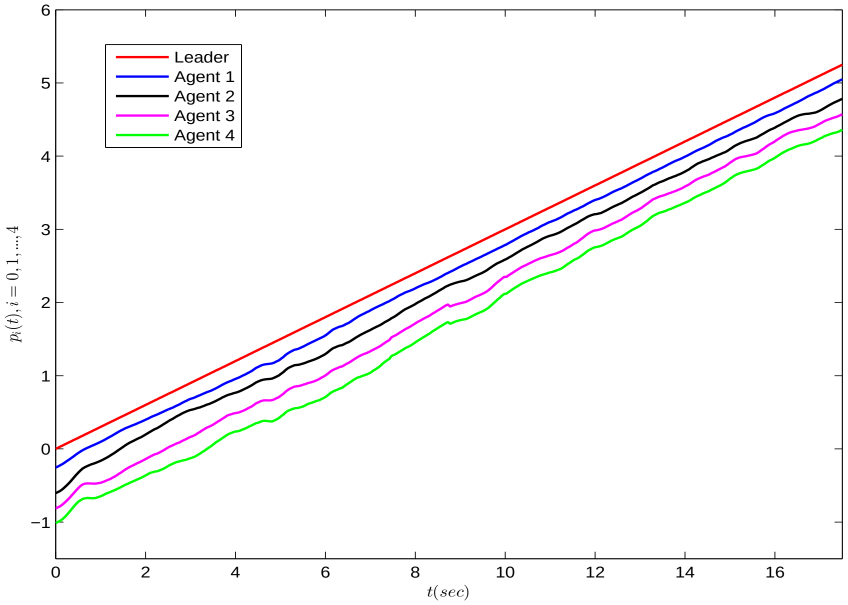

Fig. 4.4: *The position of the platoon vehicles of the experiment.*

4.2 Experimental Results

The platoon trajectory is determined by the leader node, which follows a constant velocity model given by $p_0(t) = 0.3t$ ($p \to m, t \to s$). Furthermore, the desired distance between consecutive vehicles is equally set at $\Delta_{i-1,i} = \Delta^* = 0.2$m, $i = 1, \ldots, 4$ whereas the collision and connectivity constraints are given by $\Delta_{\text{col}} = 0.05$m and $\Delta_{\text{con}} = 0.65$m respectively. Moreover, we also require steady state errors of no more than 0.1m and minimum speed of convergence as obtained by the exponential $e^{-0.5t}$. Thus, according to (3.3), we selected the parameters $\underline{M}_{p_i} = 0.15$ and $\overline{M}_{p_i} = 0.45$, $i = 1, \ldots, 4$ and the functions $\rho_{p_i}(t) = 0.78e^{-0.5t} + 0.22$, $i = 1, \ldots, 4$ in order to achieve the desired transient and steady state performance specifications as well as to comply with the collision and connectivity constraints. The control gain value was chosen as $k_p = 0.05$ to limit the desired velocities in the feasible range of the vehicle motors.

The simulation results are illustrated in Figs 4.4-4.7. More specifically, Fig. 4.4 shows the position of the vehicles with respect to time, the evolution of the neighborhood errors $e_{p_i}(t)$, $i = 1, \ldots, 4$ along with the imposed performance bounds by the corresponding performance functions are given in Fig. 4.5, while the required control inputs are illustrated in Fig. 4.6. Furthermore, Fig. 4.7 depicts the intervehicular distances along with the collision and connectivity constraints. As it was predicted by the theoretical analysis and is actually depicted in the aforementioned figures, guaranteed transient and steady state response as well as collision avoidance and connectivity maintenance are achieved with bounded closed loop signals, despite the lack of knoweldge of the vehicles' dynamics and irrespectively of the number of vehicles composing the platoon.

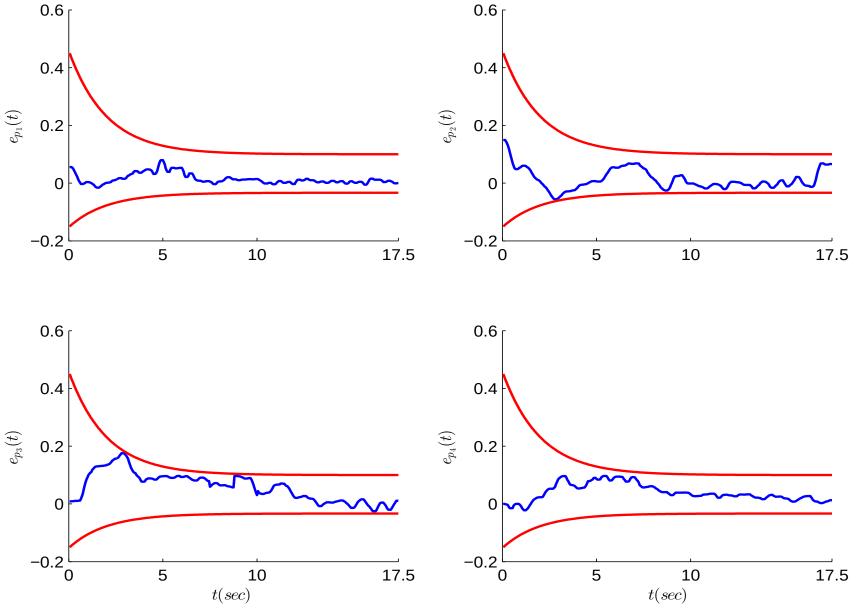

Fig. 4.5: *The evolution of the distance errors $e_{p_i}(t), i = 1, \ldots, 4$ (blue lines), along with the imposed performance bounds (red lines) for the experiment.*

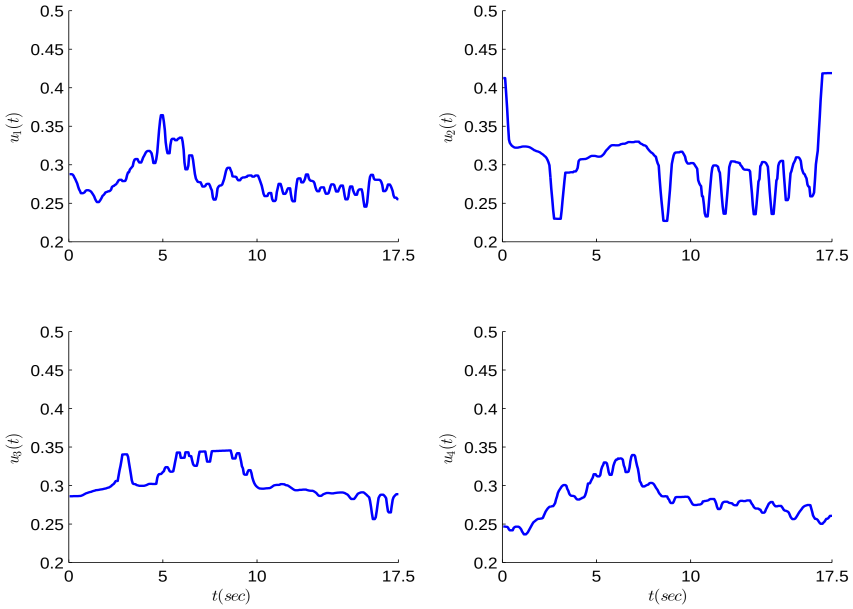

Fig. 4.6: *The required control input signals for the experiment.*

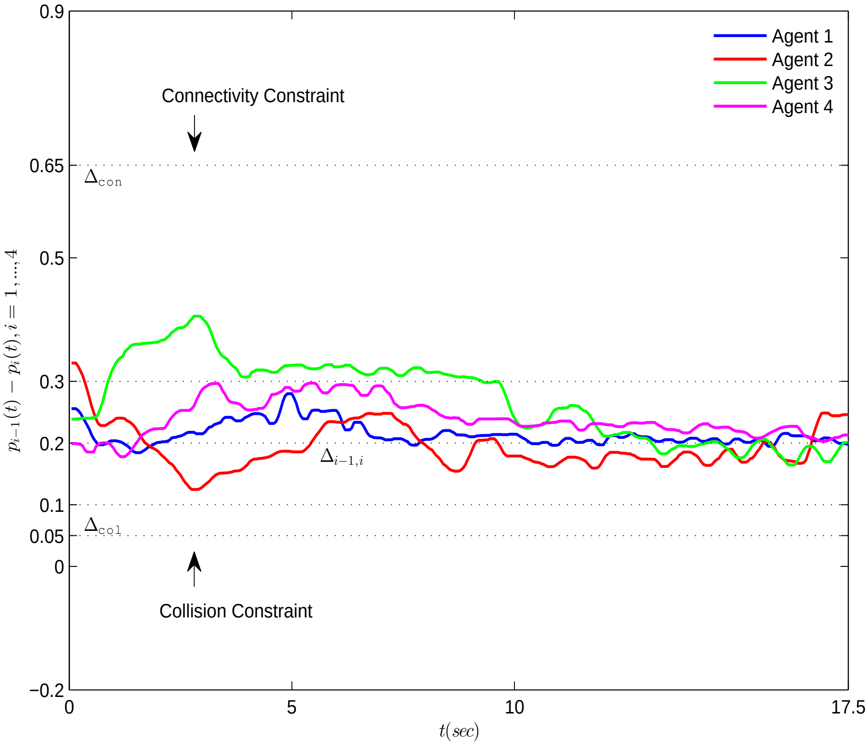

Fig. 4.7: *The distance between successive vehicles along with the collision and connectivity constraints for the experiment.*

Chapter 5

Conclusions and Future Work

5.1 Conclusion

In this work, we proposed decentralized control protocols for 1-D and 2-D vehicular platoons with unknown nonlinear dynamics. In particular, two control schemes were suggested for the $1-$dimensional case, the predecessor-following architecture, where the control action of each vehicle depends only on the relative information from its immediate predecessor, and the bidirectional architecture, where the control action depends equally upon relative measurements from both the predecessor and the follower. Similarly, we designed a control protocol for vehicular platoons moving in the 2-dimensional plane in a predecessor-following manner, since each vehicle utilizes relative information with respect to the vehicle in front of it. The aforementioned control schemes establish arbirarily fast and maintain with arbitrary accuracy a desired formation without:

- any intervehicular collisions
- violating the connectivity constraints imposed by the limited capabilities of the sensory systems.

Finally, the efficiency of the 1-dimensional case was verified by real-time experiments, whereas extensive simulation studies were conducted for both cases.

5.2 Future Work

Future research efforts will be devoted mainly for the 2-dimensional case towards:

- addressing the bidirectional architecture in a similar framework (i.e., prescribed performance as well as collision and connectivity constraints)
- guaranteeing obstacle avoidance by incorporating a $\beta_{i,des}$ parameter and adapting appropriately the value of $d_{i,des}$ without modifying the leader trajectory
- conducting real-time experiments to verify the theoretical findings.

Appendices

Appendix A′

Prescribed Performance

The control scheme is connected to the prescribed performance notion that was originally proposed to design robust state feedback controllers, for various classes of nonlinear systems [71, 72, 73], capable of guaranteeing output tracking with prescribed performance. In this work, by prescribed performance, it is meant that the output tracking error converges to a predefined arbitrarily small residual set with convergence rate no less than a certain predefined value. For completeness and compactness of presentation, this chapter summarizes preliminary knowledge on prescribed performance. In that respect, consider a generic scalar tracking error $e(t)$. Prescribed performance is achieved if $e(t)$ evolves strictly within a predefined region that is bounded by certain functions of time. The mathematical expression of prescribed performance is given by the following inequalities:

$$-\rho_L(t) < e(t) < \rho_U(t), \forall t \geq 0 \tag{A′.1}$$

where $\rho_L(t)$, $\rho_U(t)$ are smooth and bounded functions of time satisfying $\lim_{t\to\infty}\rho_U(t) > \lim_{t\to\infty}\rho_L(t)$, called performance functions. The aforementioned statements are clearly illustrated in Fig (fig) for exponential performance functions $\rho_i(t) = (\rho_{i0} - \rho_{i\infty})e^{-l_i t} + \rho_{i\infty}$ with ρ_{i0}, $\rho_{i\infty}$, l_i, $i \in \{L, U\}$ appropriately chosen constants. The constants $\rho_{L0} = \rho_L(0)$, $\rho_{U0} = \rho_U(0)$ are selected such that $\rho_{U0} > e(0) > -\rho_{L0}$ and the constants $\rho_{L\infty} = \lim_{t\to\infty}\rho_L(t)$, $\rho_{U\infty} = \lim_{t\to\infty}\rho_U(t)$ represent the maximum allowable size of the tracking error $e(t)$ at the steady state, which may even be set arbitrarily small to a value reflecting the resolution of the measurement device, thus achieving practical convergence of $e(t)$ to zero. Moreover, the decreasing rate of $\rho_L(t)$, $\rho_U(t)$ which is affected by the constants l_L, l_U in this case, introduces a lower bound on the required speed of convergence of $e(t)$. Therefore, the appropriate selection of the performance functions $\rho_L(t)$, $\rho_U(t)$ imposes performance characteristics on the tracking error $e(t)$.

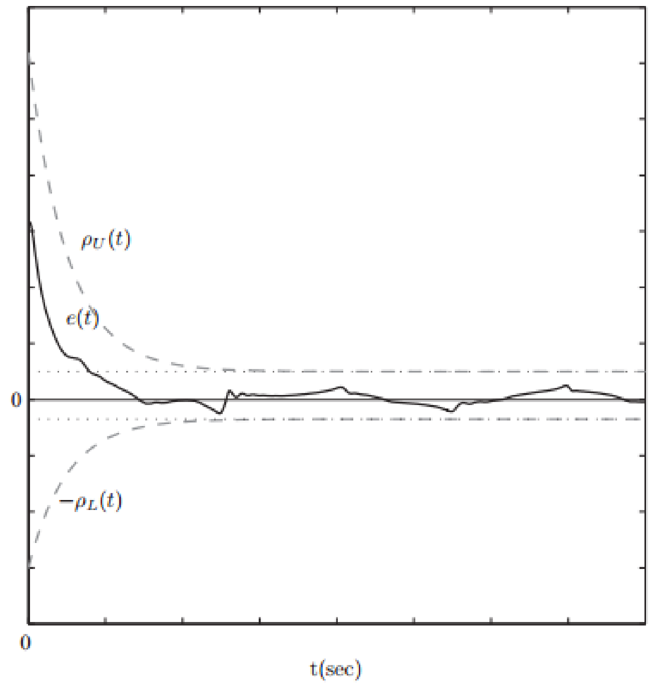

Fig. A΄.1: *Graphical illustration of the prescribed performance definition*

Appendix B′

Dynamical Systems

Consider the initial value problem:

$$\dot{\psi} = H(t, \psi),\ \psi(0) = \psi^0 \in \Omega_\psi \tag{B′.1}$$

with $H : \Re_+ \times \Omega_\psi \to \Re^n$ where $\Omega_\psi \subset \Re^n$ is a non-empty open set.

Definition 2.1. *[74] A solution $\psi(t)$ of the initial value problem (B′.1) is maximal if it has no proper right extension that is also a solution of (B′.1).*

As an example, consider the initial value problem $\dot{\psi} = \psi^2$, $\psi(0) = 1$, whose solution is $\psi(t) = \frac{1}{1-t}, \forall t \in [0, 1)$. The solution is maximal since it cannot be defined for $t > 1$. Stated otherwise, there is no proper extension of $\psi(t)$ to the right of $t = 1$ that is also a solution of the original initial value problem.

Theorem 2.3. *[74] Consider the initial value problem (B′.1). Assume that $H(t, \psi)$ is: a) locally Lipschitz on ψ for almost all $t \in \Re_+$, b) piecewise continuous on t for each fixed $\psi \in \Omega_\psi$ and c) locally integrable on t for each fixed $\psi \in \Omega_\psi$. Then, there exists a maximal solution $\psi(t)$ of (B′.1) on the time interval $[0, t_{\max})$ with $t_{\max} > 0$ such that $\psi(t) \in \Omega_\psi, \forall t \in [0, t_{\max})$.*

Proposition 2.1. *[74] Assume that the hypotheses of Theorem 2.3 hold. For a maximal solution $\psi(t)$ on the time interval $[0, t_{\max})$ with $t_{\max} < \infty$ and for any compact set $\Omega'_\psi \subset \Omega_\psi$ there exists a time instant $t' \in [0, t_{\max})$ such that $\psi(t') \notin \Omega'_\psi$.*

Βιβλιογραφία

[1] D. Swaroop and J. Hedrick, “String stability of interconnected systems,” *IEEE Transactions on Automatic Control*, vol. 41, no. 3, pp. 349–357, Mar 1996.

[2] S. M. Melzer and B. C. Kuo, “Optimal regulation of systems described by a countably infinite number of objects,” *Automatica*, vol. 7, no. 3, pp. 359–366, 1971.

[3] W. S. Levine and M. Athans, “On the optimal error regulation of a string of moving vehicles,” *IEEE Transactions on Automatic Control*, vol. 11, pp. 355–361, 1966.

[4] S. M. Melzer and B. Kuo, “A closed-form solution for the optimal error regulation of a string of moving vehicles,” *IEEE Transactions on Automatic Control*, vol. 16, no. 1, pp. 50–52, Feb 1971.

[5] S. E. Shladover, “Longitudinal control of automotive vehicles in close-formation platoons,” *Journal of Dynamic Systems, Measurement, and Control*, vol. 113, no. 2, pp. 231–241, 1991.

[6] H. . Tan, R. Rajesh, and W. . Zhang, “Demonstration of an automated highway platoon system,” in *Proceedings of the American Control Conference*, vol. 3, 1998, pp. 1823–1827.

[7] M. R. Jovanovic and B. Bamieh, “On the ill-posedness of certain vehicular platoon control problems,” *IEEE Transactions on Automatic Control*, vol. 50, no. 9, pp. 1307–1321, 2005.

[8] Z. Qu, J. Wang, and R. Hull, “Cooperative control of dynamical systems with application to autonomous vehicles,” *IEEE Transactions on Automatic Control*, vol. 53, no. 4, pp. 894–911, May 2008.

[9] R. Rajamani, H.-S. Tan, B. K. Law, and W.-B. Zhang, “Demonstration of integrated longitudinal and lateral control for the operation of automated vehicles in platoons,” *IEEE Transactions on Control Systems Technology*, vol. 8, no. 4, pp. 695–708, Jul 2000.

[10] P. Varaiya, “Smart cars on smart roads: problems of control,” *IEEE Transactions on Automatic Control*, vol. 38, no. 2, pp. 195–207, Feb 1993.

[11] J. Hedrick, M. Tomizuka, and P. Varaiya, “Control issues in automated highway systems,” *IEEE Control Systems*, vol. 14, no. 6, pp. 21–32, Dec 1994.

[12] H. Peng, "Link-layer vehicle control system for its," in *Proceedings of the 1995 American Control Conference*, vol. 1, Jun 1995, pp. 160–164 vol.1.

[13] H. Raza and P. Ioannou, "Vehicle following control design for automated highway systems," *IEEE Control Systems*, vol. 16, no. 6, pp. 43–60, Dec 1996.

[14] X. Liu, A. Goldsmith, S. Mahal, and J. Hedrick, "Effects of communication delay on string stability in vehicle platoons," in *IEEE Proceedings on Intelligent Transportation Systems, 2001*, 2001, pp. 625–630.

[15] T. S. no, K.-T. Chong, and D.-H. Roh, "A lyapunov function approach to longitudinal control of vehicles in a platoon," *IEEE Transactions on Vehicular Technology*, vol. 50, no. 1, pp. 116–124, Jan 2001.

[16] P. Y. Li, R. Horowitz, L. Alvarez, J. Frankel, and A. M. Robertson, "An automated highway system link layer controller for traffic flow stabilization," 1997.

[17] C. P. Bechlioulis, D. V. Dimarogonas, and K. J. Kyriakopoulos, "Robust control of large vehicular platoons with prescribed transient and steady state performance," in *Proceedings of the IEEE Conference on Decision and Control*, 2014, Accepted.

[18] M. E. Khatir and E. J. Davison, "Decentralized control of a large platoon of vehicles using non-identical controllers," in *Proceedings of the American Control Conference*, vol. 3, 2004, pp. 2769–2776.

[19] F. Morbidi, P. Colaneri, and T. Stanger, "Decentralized optimal control of a car platoon with guaranteed string stability," in *2013 European Control Conference (ECC)*, July 2013, pp. 3494–3499.

[20] S. S. Stankovic, M. J. Stanojevic, and D. D. Siljak, "Decentralized overlapping control of a platoon of vehicles," *IEEE Transactions on Control Systems Technology*, vol. 8, no. 5, pp. 816–832, 2000.

[21] P. Y. Li and A. Shrivastava, "Traffic flow stability induced by constant time headway policy for adaptive cruise control vehicles," *Transportation Research Part C: Emerging Technologies*, vol. 10, no. 4, pp. 275–301, 2002.

[22] C. C. Chien and P. Ioannou, "Automatic vehicle-following," in *1992 American Control Conference*, June 1992, pp. 1748–1752.

[23] D. Godbole and J. Lygeros, "Longitudinal control of the lead car of a platoon," *IEEE Transactions on Vehicular Technology*, vol. 43, no. 4, pp. 1125–1135, Nov 1994.

[24] D. Swaroop and J. K. Hedrick, "Direct adaptive longitudinal control of vehicle platoons," in *Proceedings of the IEEE Conference on Decision and Control*, vol. 1, 1994, pp. 684–689.

[25] S. Warnick and A. Rodriguez, "Longitudinal control of a platoon of vehicles with multiple saturating nonlinearities," in *1994 American Control Conference*, vol. 1, June 1994, pp. 403–407 vol.1.

[26] C.-Y. Liang and H. Peng, "Optimal adaptive cruise control with guaranteed string stability," *Vehicle System Dynamics*, vol. 32, no. 4-5, pp. 313–330, 1999. [Online]. Available: http://www.tandfonline.com/doi/abs/10.1076/vesd.32.4.313.2083

[27] A. Stotsky, C. C. Chien, and P. Ioannou, "Robust platoon-stable controller design for autonomous intelligent vehicles," in *Proceedings of the IEEE Conference on Decision and Control*, vol. 3, 1994, pp. 2431–2436.

[28] S. Klinge and R. Middleton, "Time headway requirements for string stability of homogeneous linear unidirectionally connected systems," in *Proceedings of the 48th IEEE Conference on Decision and Control, 2009 held jointly with the 2009 28th Chinese Control Conference. CDC/CCC 2009.*, Dec 2009, pp. 1992–1997.

[29] H. Hao and P. Barooah, "Stability and robustness of large platoons of vehicles with double-integrator models and nearest neighbor interaction," *International Journal of Robust and Nonlinear Control*, vol. 23, no. 18, 2013.

[30] L. E. Peppard, "String stability of relative-motion pid vehicle control systems." *IEEE Transactions on Automatic Control*, vol. AC-19, no. 5, pp. 579–581, 1974.

[31] Y. Zhang, E. B. Kosmatopoulos, P. A. Ioannou, and C. C. Chien, "Autonomous intelligent cruise control using front and back information for tight vehicle following maneuvers," *IEEE Transactions on Vehicular Technology*, vol. 48, no. 1, pp. 319–328, 1999.

[32] P. Barooah and J. P. Hespanha, "Error amplification and disturbance propagation in vehicle strings with decentralized linear control," in *Proceedings of the 44th IEEE Conference on Decision and Control, and the European Control Conference, CDC-ECC '05*, vol. 2005, 2005, pp. 4964–4969.

[33] P. Barooah, P. G. Mehta, and J. P. Hespanha, "Mistuning-based control design to improve closed-loop stability margin of vehicular platoons," *IEEE Transactions on Automatic Control*, vol. 54, no. 9, pp. 2100–2113, 2009.

[34] F. Lin, M. Fardad, and M. Jovanovic, "Optimal control of vehicular formations with nearest neighbor interactions," *IEEE Transactions on Automatic Control*, vol. 57, no. 9, pp. 2203–2218, Sept 2012.

[35] W. Khaisongkram and S. Hara, "Performance analysis of decentralized cooperative driving under non-symmetric bidirectional information architecture," in *2010 IEEE International Conference on Control Applications (CCA)*, Sept 2010, pp. 2035–2040.

[36] J. Veerman, "Stability of large flocks: an example," *arXiv preprint arXiv:1002.0768*, 2010.

[37] G. Guo and W. Yue, "Autonomous platoon control allowing range-limited sensors," *IEEE Transactions on Vehicular Technology*, vol. 61, no. 7, pp. 2901–2912, Sept 2012.

[38] S. Sheikholeslam and C. A. Desoer, “Longitudinal control of a platoon of vehicles,” in *Proceedings of the American Control Conference*, 1990, pp. 291–296.

[39] H. Koroglu and P. Falcone, “Controller synthesis for a homogenous platoon under leader and predecessor following scheme,” in *2014 American Control Conference (ACC)*, June 2014, pp. 1463–1468.

[40] S. Yadlapalli, S. Darbha, and K. R. Rajagopal, “Information flow and its relation to stability of the motion of vehicles in a rigid formation,” *IEEE Transactions on Automatic Control*, vol. 51, no. 8, pp. 1315–1319, Aug 2006.

[41] P. Seiler, A. Pant, and K. Hedrick, “Disturbance propagation in vehicle strings,” *IEEE Transactions on Automatic Control*, vol. 49, no. 10, pp. 1835–1841, 2004.

[42] K.-C. Chu, “Optimal dencentralized regulation for a string of coupled systems,” *IEEE Transactions on Automatic Control*, vol. 19, no. 3, pp. 243–246, Jun 1974.

[43] M. Jovanovic, J. Fowler, B. Bamieh, and R. D’Andrea, “On avoiding saturation in the control of vehicular platoons,” in *Proceedings of the 2004 American Control Conference, 2004.*, vol. 3, June 2004, pp. 2257–2262 vol.3.

[44] S.-Y. Han, Y.-H. Chen, L. Wang, and A. Abraham, “Decentralized longitudinal tracking control for cooperative adaptive cruise control systems in a platoon,” in *2013 IEEE International Conference on Systems, Man, and Cybernetics (SMC)*, Oct 2013, pp. 2013–2018.

[45] A. Ali, G. Garcia, and P. Martinet, “Minimizing the inter-vehicle distances of the time headway policy for urban platoon control with decoupled longitudinal and lateral control,” in *2013 16th International IEEE Conference on Intelligent Transportation Systems - (ITSC)*, Oct 2013, pp. 1805–1810.

[46] Y.-F. Peng, C.-F. Hsu, C.-M. Lin, and T.-T. Lee, “Robust intelligent backstepping longitudinal control of vehicle platoons with h infin; tracking performance,” in *IEEE International Conference on Systems, Man and Cybernetics, 2006. SMC ’06.*, vol. 6, Oct 2006, pp. 4648–4653.

[47] D. Swaroop, J. K. Hedrick, C. C. Chien, and P. Ioannou, “Comparision of spacing and headway control laws for automatically controlled vehicles,” *Vehicle System Dynamics*, vol. 23, no. 8, pp. 597–625, 1994.

[48] P. Li, L. Alvarez, and R. Horowitz, “Ahs safe control laws for platoon leaders,” *IEEE Transactions on Control Systems Technology*, vol. 5, no. 6, pp. 614–628, Nov 1997.

[49] M. Mazo, A. Speranzon, K. Johansson, and X. Hu, “Multi-robot tracking of a moving object using directional sensors,” in *2004 IEEE International Conference on Robotics and Automation, 2004. Proceedings. ICRA ’04.*, vol. 2, April 2004, pp. 1103–1108 Vol.2.

[50] G. Mariottini, G. Pappas, D. Prattichizzo, and K. Daniilidis, “Vision-based localization of leader-follower formations,” in *44th IEEE Conference on Decision and Control, 2005 and 2005 European Control Conference. CDC-ECC ’05.*, Dec 2005, pp. 635–640.

[51] T. Gustavi and X. Hu, “Formation control for mobile robots with limited sensor information,” in *Proceedings of the 2005 IEEE International Conference on Robotics and Automation, 2005. ICRA 2005.*, April 2005, pp. 1791–1796.

[52] A. Das, R. Fierro, V. Kumar, J. Ostrowski, J. Spletzer, and C. Taylor, “A vision-based formation control framework,” *IEEE Transactions on Robotics and Automation*, vol. 18, no. 5, pp. 813–825, Oct 2002.

[53] T. Gustavi and X. Hu, “Observer-based leader-following formation control using onboard sensor information,” *IEEE Transactions on Robotics*, vol. 24, no. 6, pp. 1457–1462, Dec 2008.

[54] M. Khatir and E. Davison, “A decentralized lateral-longitudinal controller for a platoon of vehicles operating on a plane,” in *American Control Conference, 2006*, June 2006, pp. 6 pp.–.

[55] M. Pham and D. Wang, “A unified nonlinear controller for a platoon of car-like vehicles,” in *Proceedings of the 2004 American Control Conference, 2004.*, vol. 3, June 2004, pp. 2350–2355 vol.3.

[56] H. Tanner, G. Pappas, and V. Kumar, “Leader-to-formation stability,” *IEEE Transactions on Robotics and Automation*, vol. 20, no. 3, pp. 443–455, June 2004.

[57] J. Lawton, R. Beard, and B. Young, “A decentralized approach to formation maneuvers,” *IEEE Transactions on Robotics and Automation*, vol. 19, no. 6, pp. 933–941, Dec 2003.

[58] D. Maithripala, J. Berg, D. Maithripala, and S. Jayasuriya, “A geometric virtual structure approach to decentralized formation control,” in *American Control Conference (ACC), 2014*, June 2014, pp. 5736–5741.

[59] R. Vidal, O. Shakernia, and S. Sastry, “Formation control of nonholonomic mobile robots with omnidirectional visual servoing and motion segmentation,” in *IEEE International Conference on Robotics and Automation, 2003. Proceedings. ICRA ’03.*, vol. 1, Sept 2003, pp. 584–589 vol.1.

[60] H. Hao, P. Barooah, and P. G. Mehta, “Distributed control of two dimensional vehicular formations: stability margin improvement by mistuning,” in *ASME 2009 Dynamic Systems and Control Conference*. American Society of Mechanical Engineers, 2009, pp. 699–706.

[61] D. Panagou and V. Kumar, “Cooperative visibility maintenance for leader–follower formations in obstacle environments,” *IEEE Transactions on Robotics*, vol. 30, no. 4, pp. 831–844, Aug 2014.

[62] N. Cowan, O. Shakerina, R. Vidal, and S. Sastry, “Vision-based follow-the-leader,” in *Proceedings. 2003 IEEE/RSJ International Conference on Intelligent Robots and Systems, 2003. (IROS 2003).*, vol. 2, Oct 2003, pp. 1796–1801 vol.2.

[63] G. Mariottini, F. Morbidi, D. Prattichizzo, G. Pappas, and K. Daniilidis, “Leader-follower formations: Uncalibrated vision-based localization and control,” in *2007 IEEE International Conference on Robotics and Automation*, April 2007, pp. 2403–2408.

[64] G. Mariottini, F. Morbidi, D. Prattichizzo, N. Vander Valk, N. Michael, G. Pappas, and K. Daniilidis, “Vision-based localization for leader 2013;follower formation control,” *IEEE Transactions on Robotics*, vol. 25, no. 6, pp. 1431–1438, Dec 2009.

[65] Z. Qu, *Cooperative Control of Dynamical Systems: Applications to Autonomous Vehicles*. New York, USA: Springer, 2009.

[66] A. Berman and R. J. Plemmons, *Nonnegative Matrices in the Mathematical Science*, ser. Classics in Applied Mathematics. Philadelphia, USA: SIAM, 1994.

[67] E. Ivanjko, T. Petrinic, and I. Petrovic, “Modelling of mobile robot dynamics,” in *7th EUROSIM Congress on Modelling and Simulation*, vol. 2, 2007.

[68] C. P. Bechlioulis and G. A. Rovithakis, “A low-complexity global approximation-free control scheme with prescribed performance for unknown pure feedback systems,” *Automatica*, vol. 50, no. 4, pp. 1217–1226, 2014.

[69] W. . Yueh and S. S. Cheng, “Explicit eigenvalues and inverses of tridiagonal toeplitz matrices with four perturbed corners,” *ANZIAM Journal*, vol. 49, no. 3, pp. 361–387, 2008.

[70] Webots, “http://www.cyberbotics.com,” commercial Mobile Robot Simulation Software. [Online]. Available: http://www.cyberbotics.com

[71] C. P. Bechlioulis and G. A. Rovithakis, “Robust adaptive control of feedback linearizable mimo nonlinear systems with prescribed performance,” *IEEE Transactions on Automatic Control*, vol. 53, no. 9, pp. 2090–2099, 2008.

[72] ——, “Adaptive control with guaranteed transient and steady state tracking error bounds for strict feedback systems,” *Automatica*, vol. 45, no. 2, pp. 532–538, 2009.

[73] ——, “Prescribed performance adaptive control for multi-input multi-output affine in the control nonlinear systems,” *IEEE Transactions on Automatic Control*, vol. 55, no. 5, pp. 1220–1226, 2010.

[74] E. D. Sontag, *Mathematical Control Theory*. London, U.K.: Springer, 1998.